Mathematics

https://www.aimspress.com/journal/Math

AIMS Mathematics, 11(6): 19338–19378.
DOI: 10.3934/math.2026786
Received: 10 April 2026
Revised: 22 June 2026
Accepted: 24 June 2026
Published: 30 June 2026

Research article

The evaluation of two vulnerable powered options under a general stochastic volatility jump diffusion model using a Laplace–Fourier transform

Libin Wang* **and Ruonan Zhang**

Hebei Key Laboratory of Financial Technology Application, Hebei Finance University, No. 3188, Hengxiang North Street, Baoding, Hebei, China

* **Correspondence:** wanglibin@hbfu.edu.cn.

Abstract: This paper investigates the pricing problem of two vulnerable powered options under the condition that the underlying assets price mechanism satisfies general stochastic volatility, stochastic interest rate, and stochastic jump. Specifically, a Laplace transform is first applied to simplify the payoff function of the vulnerable powered options into the product form of key term and beta function. Second, the total differentiation technique of multivariate functions is implemented to approximate the nonlinear partial differential equation group into a linear equation group, and the affine structure method is adopted to obtain the approximate joint characteristic function of log-price. Third, under the inverse Fourier transform, the approximate semi-analytical solutions of the key term are derived. Finally, the combination algorithm of discrete Laplace transform and Fourier transform is constructed to obtain the asymptotic solutions of two vulnerable powered options, and the effectiveness and stability of the pricing method are verified by numerical examples. Experimental results show that the model constructed in this paper can well reflect the laws of the real market, and the proposed method can deal with the pricing problem of vulnerable powered options efficiently.

Keywords: stochastic interest rate; stochastic volatility; Laplace–Fourier transform
Mathematics Subject Classification: 60G44, 60H30, 60J70

1. Introduction

With the accelerating pace of international economic and financial integration, combined with local wars, the COVID-19 pandemic and other emergencies, financial markets of various countries have become more interconnected, resulting in increasing financial systemic risks, especially the default risk of counterparties [1]. As a combination of financial derivatives, vulnerable options [2, 3] can not only be used as an investment object for investors, but also as a hedging tool for various underlying assets, which have been favored by the financial practice. On the other hand, as a type of high-yield financial products, various powered options have long been sought after by investors with a risk appetite. However, unfortunately, powered options are more prone to the risk of default. Therefore, this paper proposes vulnerable powered options with default risk, and obtains pricing results through a series of methods.

In many studies of option derivatives, the pricing of power and powered options is always a challenging research area. First, compared with ordinary options, power and powered options have certain financial leverage, which can enable investors to obtain more and greater excess returns. Therefore, power and powered options are more attractive in the long run. Second, power and powered options can effectively hedge the nonlinear risk of financial markets. Third, power and powered options have a large number of other applications in finance; refer to [4, 5] for details.

There has been some research on pricing methods for power and powered options. It can be traced back to Heynen and Kat [6], who derived an analytical solution for powered options under the assumptions of the standard Black–Scholes (B–S) formulation [7]. Andersen and Piterbarg [8] deeply discussed the existence and expression formula of the finite moment of the underlying asset price under the stochastic volatility model, which made valuable theoretical preparation for the pricing of power and powered options under stochastic volatility. Esser [9] derived the semi-closed solution of the powered option and its variant price in a more general framework. Kim [10] obtained the analytical closed solution of the power and powered options under the Heston model [11] and constructed the corresponding numerical pricing method to obtain the fast pricing solution. Similarly, under the Heston model, Ibrahim [12] applied the risk-neutral pricing principle to demonstrate the partial differential equation (PDE) satisfied by the powered options and obtained the asymptotic solution of the option by a fast Fourier Transform. Kim [13] first studied the pricing method of the powered options in the scenario with a regime–switching mechanism, and obtained the display expression of the price by the Laplace transform. Subsequently, Kim [14] also applied the Laplace transform to derive the pricing formula of the powered option under four different scenarios of stochastic volatility, stochastic interest rate, regime switching mechanism, and Levy process, and analyzed the convergence of the Laplace transform. In recent studies, many scholars have conducted further research on the pricing of vulnerable options and powered options. Notably, Elham [15] discussed the analytical pricing problem of powered options based on the assumption of a fractional stochastic volatility model. Xie [16] assumed that the mean reversion levels of the variance and interest rate processes were controlled by a continuous Markov process with a finite–state space when researching the pricing of vulnerable options. The model also considered the impacts of volatility risk, interest rate risk, and regime–switching risk. Han [17] constructed a two-factor stochastic volatility model and incorporated interest rate risk with regime–switching risk simultaneously. They not only solved the analytical valuation problem of powered options, but also conducted empirical research on the two-factor stochastic volatility model in the financial market. Wang [18] studied the valuation problem of vulnerable reset options under a stochastic volatility jump-diffusion model and obtained the analytical formula of the corresponding option by designing a triple–fast Fourier transform. Both theoretical analysis and numerical examples demonstrated the practicality of this method.

A large number of empirical studies have demonstrated that the prices of underlying assets experience sudden jumps, and volatility exhibits heteroskedasticity and smile phenomena. Regarding the pricing and investment issues of financial derivatives related to multiple assets, through extensive empirical research, Christoffersen [19] found that the volatility of assets is influenced by multiple market volatility factors and constructed a multifactor stochastic volatility system. Inspired by his empirical studies, this paper builds a two-factor general stochastic volatility model and incorporates macro and micro volatility factors to describe the volatility evolution of two assets. At the same time, in research on the stock price mechanism, Lian [20] discovered that asset prices exhibit asymmetric co-jumps. This phenomenon results from the varying degrees of sensitivity of different assets to market information. Based on this viewpoint, dependent jump structure is incorporated to depict the comprehensive jump phenomenon of the underlying assets in this paper. Additionally, with the development and design of credit default financial products (CDS) in China, the structure of vulnerable powered options has been applied in numerous wealth management products and quantitative investment products, such as the Healthy Wealth Management Fund No.3 launched by China CITIC Bank and the Guo-Tai-Jun-An Quantitative Investment Happiness Index Fund V, whose core is the structure of powered options with default risk. Therefore, the main research content of this paper is the semi-analytical pricing problem of vulnerable powered options based on the two-factor general stochastic volatility model. In the recent research on advanced technologies for solving high-dimensional financial partial differential equations, Liu, Soleymani, and MaliK [21] proposed a numerical method. Through the integration of inverse quadratic kernels, they explored the asymptotic pricing problem of high-dimensional multi-asset options, aiming to achieve asset portfolio diversification and thereby reduce the systemic risk of financial derivatives. Liu, Li, and MaliK [22] studied the high-dimensional option pricing problem. They used the integration of Gaussian radial basis functions to generate radial basis functions and derived the error equation, proving the applicability and practicality of the approximate pricing function. Based on this, Liu [23] explored a new method for risk assessment of financial products, using the Rayleigh distribution to calculate value at risk (VaR) and expected shortfall (ES), and conducted an empirical analysis on real-world stock data. Liu et al. [24] valued European options under the price mechanism of the Bates stochastic volatility jump diffusion process using an improved multiparticle kernel radial basis function finite difference (RBF-FD) method, and verified its significant advantages compared to the classical methods. Liu and Ding [25], based on TensorFlow, utilized a kernel-based approximation method to obtain time-dependent partial differential equations, highlighting the potential of this approach in solving partial differential equations in regular regions.

In order to describe the time-varying characteristics, this paper proposes a comprehensive price evolution mechanism of underlying assets based on a radical process with reverting property and then deduces the option pricing formula with explicit solution. The main innovations of this paper are as follows. First, a general process is applied to characterize the stochastic volatility [8], the stochastic interest rate [26], and the stochastic jump [27, 28]. Second, a combined the Laplace-Fourier algorithm is proposed to obtain the asymptotic solution of vulnerable powered options. The remaining parts of this paper are organized as follows. Section 2 gives the mathematical description of the asset price mechanism and some preparatory results of pricing, including the Laplace transform. The approximate semi-analytical solution of the key term of pricing is deduced by measure transformation and decomposition technology in Section 3. The combination algorithm of the Laplace–Fourier transform is constructed, and the asymptotic pricing formula of the vulnerable powered option is shown in Section 4. In Section 5, numerical examples are used to check the effect of the pricing method. Finally, the main innovations and methods of this paper are summarized and prospected.

2. Asset price dynamics and preliminary results

In this section, we first establish the integrated price mechanism of underlying asset and the counterparty's asset along with the evolution path of interest rate based on a general stochastic volatility model, and we carry out a detailed mathematical description. Then, the Laplace transform is applied to simplify the pricing formula of vulnerable powered options, and the joint characteristic function of log-asset prices are further constructed, which makes theoretical preparation for the pricing of vulnerable powered options in the next step. Based on the work of Heston [11], the existence and transformation of risk-neutral measures in a stochastic volatility environment are demonstrated. Merton [27] explained the risk-neutral measure and measure transformation formula under the compound Poisson jump process, and Hull and White [29] provided the risk-neutral measure in a stochastic interest rate environment. Therefore, in this paper, based on these three aspects, we directly construct the following price mechanism for two assets under the risk-neutral measure.

Let $s_{it}(i = 1, 2)$ be the value of underlying assets at time t satisfying the following stochastic differential equation under risk neutral measure $\mathbb{Q}$,

$$\begin{aligned}
\frac{ds_{1t}}{s_{1t}} &= (r_t - \lambda_0 m_{01} - \lambda_1 m_{11})dt + f(v_{1t}, v_{2t})dW_{1t} + (e^{J_{01}} - 1)dN_{0t} + (e^{J_{11}} - 1)dN_{1t}, && (2.1)\\
\frac{ds_{2t}}{s_{2t}} &= (r_t - \lambda_0 m_{02} - \lambda_2 m_{12})dt + g(v_{1t}, v_{2t})dW_{2t} + (e^{J_{02}} - 1)dN_{0t} + (e^{J_{12}} - 1)dN_{2t}, && (2.2)\\
dv_{1t} &= k_1(\theta_1 - v_{1t})dt + \sigma_1 v_{1t}^{\alpha} dW_{1t}^{(v)}, 0 \le \alpha \le 1, && (2.3)\\
dv_{2t} &= k_2(\theta_2 - v_{2t})dt + \sigma_2 v_{2t}^{\beta} dW_{2t}^{(v)}, 0 \le \beta \le 1, && (2.4)\\
dr_t &= k_r(\theta_r - r_t)dt + \sigma_r r_t^{\gamma} dW_{rt}, 0 \le \gamma \le 1, && (2.5)
\end{aligned}$$

where r_t is the riskless interest rate, $f(v_{1t}, v_{2t})$ and $g(v_{1t}, v_{2t})$ are the volatility functions of the assets, and $v_{it}(i = 1, 2)$ are the impact factors of assets volatility. It is clear that r_t and v_{it} are diffusion processes with a reverting nature. Here, σ_1, σ_2, and σ_r are positive coefficients of diffusion; k_1, k_2, and k_r are positive coefficients of a mean-reversion speed; and θ_1, θ_2, and θ_r are positive coefficients of mean level. α, β, γ are coefficients of variation of the model. If $\alpha = 0$, or $\beta = 0$, or $\gamma = 0$, the processes are the Ornstein–Uhlenbeck processes with additive noise; if $\alpha = \frac{1}{2}$, or $\beta = \frac{1}{2}$, or $\gamma = \frac{1}{2}$, the processes are the Cox–Ingeroll–Ross (CIR)/Heston variance models. For the positivity of v_{1t}, v_{2t}, and r_t, by applying the invariant distribution of v_{1t}, v_{2t}, and r_t, the positivity conditions for v_{1t}, v_{2t}, and r_t will be presented in Appendix.

The assumptions of Brownian motion and Poisson processes are given in the following part. First, assume that all Brownian motions are independent of all Poisson processes. The correlation structure of the Brownian motions involved in the above model is presented by

$$\begin{aligned}
&d\langle W_{1t}, W_{2t}\rangle = \rho_{12}dt, d\langle W_{1t}, W_{1t}^{(v)}\rangle = \rho_{1v_1}dt, , d\langle W_{1t}, W_{2t}^{(v)}\rangle = \rho_{1v_2}dt,\\
&d\langle W_{2t}, W_{1t}^{(v)}\rangle = \rho_{2v_1}dt, , d\langle W_{2t}, W_{2t}^{(v)}\rangle = \rho_{2v_2}dt,
\end{aligned}$$

where ρ_{12} indicates the correlation coefficient of the two assets (s_{1t}, s_{2t}), ρ_{1v_1} indicates the correlation coefficient of the asset s_{1t} and the random volatility factor v_{1t}, ρ_{1v_2} indicates the correlation coefficient of the asset s_{1t} and the random volatility factor v_{2t}, ρ_{2v_1} indicates the correlation coefficient of the asset

s_{2t} and the random volatility factor v_{1t}, and ρ_{2v_2} indicates the correlation coefficient of the asset s_{2t} and the random volatility factor v_{2t}. All other Brownian motions are independent of each other. $(\lambda_0, \lambda_1, \lambda_2)$ denotes the intensity of the Poisson process (N_{0t}, N_{1t}, N_{2t}). $m_{01} = E[e^{J_{01}} - 1]$, $m_{02} = E[e^{J_{02}} - 1]$, $m_{11} = E[e^{J_{11}} - 1]$, and $m_{12} = E[e^{J_{12}} - 1]$ are the average jump amplitude. The co-jump vectors (J_{01}, J_{02}) are subject to a two-dimensional joint normal distribution $N(\mu_1, \mu_2; \sigma^2_{J_{01}}, \sigma^2_{J_{02}}; \rho_{J_1J_2})$, where μ_1 and μ_2 are the mean of the jumps (J_{01}, J_{02}), $\sigma^2_{J_{01}}$ and $\sigma^2_{J_{02}}$ are the variance of the jumps (J_{01}, J_{02}), and $\rho_{J_1J_2}$ is the correlation coefficient of the jumps (J_{01}, J_{02}). The personality jump variables $J_{1i}(i = 1, 2)$ are asymmetric double exponential distribution with the following density:

$$f_{J_{1i}} = p_i \xi_i e^{\xi_i x} 1_{\{x<0\}} + q_i \eta_i e^{-\eta_i x} 1_{\{x>0\}}, p_i + q_i = 1,$$

where q_1 and q_2 represent the positive jump probability of the logarithm of the jumps J_{11} and J_{12}, η_1 and η_2 represent the positive jump attenuation coefficient of the logarithm of the jumps J_{11} and J_{12}, p_1 and p_2 represent the negative jump probability of the logarithm of the jumps J_{11} and J_{12}, and ξ_1 and ξ_2 represent the negative jump attenuation coefficient of the logarithm of the jumps J_{11} and J_{12}.

The following presents the structural decomposition of the price processes of the two assets (s_{1t}, s_{2t}) to illustrate that the asset prices satisfy the condition of being discounted as a martingale. By reorganizing the price processes of the two assets, we can obtain

$$\begin{aligned}
\frac{ds_{1t}}{s_{1t}} &= r_t dt + f(v_{1t}, v_{2t}) dW_{1t} + [(e^{J_{01}} - 1) dN_{0t} - \lambda_0 m_{01} dt] + [(e^{J_{11}} - 1) dN_{1t} - \lambda_1 m_{11} dt], \\
\frac{ds_{2t}}{s_{2t}} &= r_t dt + g(v_{1t}, v_{2t}) dW_{2t} + [(e^{J_{02}} - 1) dN_{0t} - \lambda_0 m_{02} dt] + [(e^{J_{12}} - 1) dN_{2t} - \lambda_2 m_{12} dt].
\end{aligned}$$

It can be clearly seen that the price processes (s_{1t}, s_{2t}) of both assets can be decomposed into the drift process of interest rates, the continuous martingale process, and the sum of two compensatory compound Poisson processes (jump martingale processes). Therefore, (s_{1t}, s_{2t}) meet the condition of discounting to martingales.

It should be noted that the core economic basis for this paper to adopt the mean reversion process for volatility and interest rate modeling lies in the fact that the fluctuations in asset prices and interest rates are essentially the market's response to information shocks. When new information or unexpected events occur, the market enters a state of high volatility; when the information is fully digested by the market (and prices fully reflect that fact), the fluctuations naturally subside and return to the normal level without significant information. From the perspective of behavioral finance, when asset price fluctuations or interest rates are abnormally high, it usually corresponds to extreme emotions such as panic or frenzy, and the emotions will gradually return to rationality over time, and the fluctuations will converge. When asset prices or interest rates are abnormally low, they often correspond to a lackluster market transaction, but as new information accumulates, the fluctuations will naturally rise back to the normal level. In addition, the market's own supply and demand balance mechanism will push volatility and interest rates toward the long-term average level.

In this work, the payoff function of two vulnerable powered options is given by $h(s_{1T}, s_{2T})$. The payoff function of the m-th powered European (call or put) options is given by

$$h_1^+(s_{1T}, s_{2T}) = (s_{1T} - K)^m \cdot 1_{\{s_{1T}>K\}} \cdot (1_{\{s_{2T} \geq D^*\}} + \frac{(1-\varpi)s_{2T}}{D} 1_{\{s_{2T}<D^*\}}), \tag{2.6}$$

$$h_1^-(s_{1T}, s_{2T}) = (K - s_{1T})^m \cdot 1_{\{s_{1T}<K\}} \cdot (1_{\{s_{2T}\geq D^*\}} + \frac{(1-\varpi)s_{2T}}{D} 1_{\{s_{2T}<D^*\}}); \tag{2.7}$$

the payoff function of the m-th powered forward start (call or put) options is given by

$$h_2^+(s_{1T}, s_{2T}) = (s_{1T} - Ks_{1t^*})^m \cdot 1_{\{s_{1T}>Ks_{1t^*}\}} \cdot (1_{\{s_{2T}\geq D^*\}} + \frac{(1-\varpi)s_{2T}}{D} 1_{\{s_{2T}<D^*\}}), \tag{2.8}$$

$$h_2^-(s_{1T}, s_{2T}) = (Ks_{1t^*} - s_{1T})^m \cdot 1_{\{s_{1T}<Ks_{1t^*}\}} \cdot (1_{\{s_{2T}\geq D^*\}} + \frac{(1-\varpi)s_{2T}}{D} 1_{\{s_{2T}<D^*\}}), \tag{2.9}$$

where t^* is the base moment of forward options, and $t^* \in [t, T]$. Further, s_{2T} is the market value of the counterpart asset s_{1T} at maturity time T, D denotes the total debt of the option writer, and ϖ represents the dead weight costs associated with the financial stress and is described as a percentage of the counterpart value. D^* is the default boundary such that a default event occurs when $s_{2T} < D^*$. The payoff function of the vulnerable option is the payoff function of the European option if $s_{2T} \geq D^*$.

Let $s_t = (s_{1t}, s_{2t})$,$s = (s_1, s_2)$,$v_t = (v_{1t}, v_{2t})$,$v = (v_1, v_2)$. According to the risk-neutral pricing principle, the pricing formula of various vulnerable powered options can be obtained as follows:

$$\begin{aligned}
C_1(t,T,m,K|s,v,r) = & \; E^{\mathbb{Q}}[e^{-\int_t^T r_s ds} h_1^+(s_{1T}, s_{2T})|s_t = s, v_t = v, r_t = r],\\
P_1(t,T,m,K|s,v,r) = & \; E^{\mathbb{Q}}[e^{-\int_t^T r_s ds} h_1^-(s_{1T}, s_{2T})|s_t = s, v_t = v, r_t = r],\\
C_2(t,T,m,K|s,v,r) = & \; E^{\mathbb{Q}}[e^{-\int_t^T r_s ds} h_2^+(s_{1T}, s_{2T})|s_t = s, v_t = v, r_t = r],\\
P_2(t,T,m,K|s,v,r) = & \; E^{\mathbb{Q}}[e^{-\int_t^T r_s ds} h_2^-(s_{1T}, s_{2T})|s_t = s, v_t = v, r_t = r].
\end{aligned} \tag{2.10}$$

Let $k = \ln K$. At the same time, by applying the Laplace transform to variable k, the following formula can be defined:

$$\begin{aligned}
C_1^*(t,T,m,w|s,v,r) = & \int_{-\infty}^{+\infty} e^{-wk} C_1(t,T,m,e^k|s,v,r)dk,\\
P_1^*(t,T,m,w|s,v,r) = & \int_{-\infty}^{+\infty} e^{-wk} P_1(t,T,m,e^k|s,v,r)dk,\\
C_2^*(t,T,m,w|s,v,r) = & \int_{-\infty}^{+\infty} e^{-wk} C_2(t,T,m,e^k|s,v,r)dk,\\
P_2^*(t,T,m,w|s,v,r) = & \int_{-\infty}^{+\infty} e^{-wk} P_2(t,T,m,e^k|s,v,r)dk.
\end{aligned} \tag{2.11}$$

Due to the commutativity of the integral and the expectation operation, the following reduction expression can be derived:

$$\begin{aligned}
& C_1^*(t,T,m,w|s,v,r) = \int_{-\infty}^{+\infty} e^{-wk} C_1(t,T,m,e^k|s,v,r)dk\\
= & \; E^{\mathbb{Q}}[e^{-\int_t^T r_s ds}(1_{\{s_{2T}\geq D^*\}} + \tfrac{1-\varpi}{D} s_{2T} 1_{\{s_{2T}<D^*\}}) \cdot \int_{-\infty}^{+\infty} e^{-wk}((s_{1T} - e^k)^m)^+ dk|\mathcal{F}_t].
\end{aligned}$$

Let $x = \frac{e^k}{s_{1T}}$. Plug in the second term inside the expectation, which can be further obtained as

$$\begin{aligned}
& \int_{-\infty}^{+\infty} e^{-wk}((s_{1T} - e^k)^m)^+ dk = \int_{-\infty}^{\ln s_{1T}} e^{-wk}(s_{1T} - e^k)^m dk\\
= & \; s_{1T}^m \int_{-\infty}^{\ln s_{1T}} e^{-wk}(1 - e^{k-\ln s_{1T}})^m dk = s_{1T}^{m-w} \cdot \int_0^1 x^{-w-1}(1-x)^{m+1-1} dx\\
= & \; s_{1T}^{m-w} \cdot B(-w, m+1), Re(w) < 0, m > -1.
\end{aligned}$$

Then, under the condition that $E^{\mathbb{Q}}[e^{-\int_t^T r_s ds} s_{1T}^{m-w}]$ is bounded, we can derive

$$C_1^*(t,T,m,w|s,v,r) = B(-w, m+1) \cdot V_1(t,T,m,w|s,v,r), Re(w) < 0, m > -1, \tag{2.12}$$

where the key item becomes

$$V_1(t,T,m,w|s,v,r) = E^{\mathbb{Q}}[e^{-\int_t^T r_s ds} s_{1T}^{m-w}(1_{\{s_{2T}\geq D^*\}} + \tfrac{1-\varpi}{D} s_{2T} 1_{\{s_{2T}<D^*\}})|\mathcal{F}_t]. \tag{2.13}$$

Similarly, under the condition that $E^{\mathbb{Q}}[e^{-\int_t^T r_s ds} s_{1T}^{m-w}|\mathcal{F}_t]$ is bounded,

$$P_1^*(t,T,m,w|s,v,r) = B(w-m, m+1)\cdot V_1(t,T,m,w|s,v,r), Re(w) > m, m > -1. \tag{2.14}$$

Under the condition that $E^{\mathbb{Q}}[e^{-\int_t^T r_s ds} s_{1T}^{m-w} s_{1t^*}^{w}|\mathcal{F}_t]$ is bounded,

$$\begin{aligned} C_2^*(t,T,m,w|s,v,r) &= B(-w, m+1)\cdot V_2(t,T,m,w|s,v,r), Re(w) < 0, m > -1; && (2.15)\\ P_2^*(t,T,m,w|s,v,r) &= B(w-m, m+1)\cdot V_2(t,T,m,w|s,v,r), Re(w) > m, m > -1, && (2.16)\end{aligned}$$

where the key item becomes

$$V_2(t,T,m,w|s,v,r) = E^{\mathbb{Q}}[e^{-\int_t^T r_s ds} s_{1T}^{m-w} s_{1t^*}^{w}(1_{\{s_{2T}\geq D^*\}} + \tfrac{1-\varpi}{D} s_{2T} 1_{\{s_{2T}<D^*\}})|\mathcal{F}_t]. \tag{2.17}$$

To ensure the existence of the Laplace transform, define the moment generating function of log-price of the underlying asset with a discounted term

$$M(t,T,y_1,v,r,n) = E^{\mathbb{Q}}[e^{-\int_t^T r_s ds} s_{1T}^{n}|\mathcal{F}_t]. \tag{2.18}$$

Below, the approximate solution of $M(t,T,y_1,v,r,n)$ is derived in Lemmas 2.1 and 2.2, which shows that $M(t,T,y_1,v,r,n)$ satisfies the condition of boundedness.

From a formal perspective, Lemma 2.1 below provides the risk-neutral price of a forward contract whose underlying asset price index is the maturity-day return. Due to the high leverage nature of the price index itself, combined with the effect of the two market volatility factors on the asset volatility, the jump risk brought about by the dependent jump structure, and the interference of the stochastic interest rate, the above forward contract price is prone to be nonexistent. Therefore, in order to ensure the reliability of the subsequent pricing of the vulnerable powered options, based on the risk-neutral pricing principle and using the technique of partial differential equations, Lemma 2.1 derived the approximate semi-analytical solution of the forward price. At the same time, Lemma 2.2 further obtained the sufficient conditions for the existence of the forward price through classification discussion, ultimately establishing the subsequent option pricing work on a solid theoretical basis.

Lemma 2.1. *Suppose that the dynamics of process s_{1t} are a general stochastic volatility process given by Eqs (2.1)–(2.5), all parameters of the pricing model satisfy the conditions stated in Lemma 2.2, and a linearization method is employed. Then an approximate solution of $M(t,T,y_1,v,r,n)$ is given by*

$$e^{ny_1+\widetilde{A}(\tau,n)+\widetilde{C}_1(\tau,n)v_1+\widetilde{C}_2(\tau,n)v_2+\widetilde{D}(\tau,n)r}, \tag{2.19}$$

where the option contract period $\tau = T-t$, $\widetilde{A}(\tau,n)$ is the coefficient of the constant term, $\widetilde{C}_1(\tau,n)$ is the coefficient of the stochastic volatility factor v_1, $\widetilde{C}_2(\tau,n)$ is the coefficient of the stochastic volatility factor v_2, and $\widetilde{D}(\tau,n)$ is the coefficient of the interest rate factor r.

$\widetilde{A}(\tau,n)$, $\widetilde{C}_1(\tau,n)$, $\widetilde{C}_2(\tau,n)$ and $\widetilde{D}(\tau,n)$ are given by

$$
\begin{aligned}
&\widetilde{A}(\tau,n) = \tilde{a}_0(n)\tau + \widetilde{a}_1(n)\widetilde{A}_1(\tau,n) + \widetilde{a}_2(n)\widetilde{A}_2(\tau,n) + \widetilde{a}_3(n)\widetilde{A}_3(\tau,n) + \widetilde{A}_4(\tau,n),\\
&\widetilde{C}_1(\tau,n) = \tfrac{\widetilde{b}_1(n)+\sqrt{\widetilde{\delta}_1(n)}}{2\alpha\sigma_1^2\theta_1^{2\alpha-1}} \cdot \tfrac{1-e^{\sqrt{\widetilde{\delta}_1(n)}\tau}}{1-\widetilde{g}_1(n)e^{\sqrt{\widetilde{\delta}_1(n)}\tau}},\\
&\widetilde{C}_2(\tau,n) = \tfrac{\widetilde{b}_2(n)+\sqrt{\widetilde{\delta}_2(n)}}{2\beta\sigma_2^2\theta_2^{2\beta-1}} \cdot \tfrac{1-e^{\sqrt{\widetilde{\delta}_2(n)}\tau}}{1-\widetilde{g}_2(n)e^{\sqrt{\widetilde{\delta}_2(n)}\tau}},\\
&\widetilde{D}(\tau,n) = \tfrac{\widetilde{b}_r(n)+\sqrt{\widetilde{\delta}_r(n)}}{2\gamma\sigma_r^2\theta_r^{2\gamma-1}} \cdot \tfrac{1-e^{\sqrt{\widetilde{\delta}_r(n)}\tau}}{1-\widetilde{g}_r(n)e^{\sqrt{\widetilde{\delta}_r(n)}\tau}}.\\
&\widetilde{A}_1(\tau,n) = \tfrac{1}{2\alpha\sigma_1^2\theta_1^{2\alpha-1}}[(\widetilde{b}_1(n) + \sqrt{\widetilde{\delta}_1(n)})\tau - 2\ln(\tfrac{1-\widetilde{g}_1(n)e^{\sqrt{\widetilde{\delta}_1(n)}\tau}}{1-\widetilde{g}_1(n)})],\\
&\widetilde{A}_2(\tau,n) = \tfrac{1}{2\beta\sigma_2^2\theta_2^{2\beta-1}}[(\widetilde{b}_2(n) + \sqrt{\widetilde{\delta}_2(n)})\tau - 2\ln(\tfrac{1-\widetilde{g}_2(n)e^{\sqrt{\widetilde{\delta}_2(n)}\tau}}{1-\widetilde{g}_2(n)})],\\
&\widetilde{A}_3(\tau,n) = \tfrac{1}{2\gamma\sigma_r^2\theta_r^{2\gamma-1}}[(\widetilde{b}_r(n) + \sqrt{\widetilde{\delta}_r(n)})\tau - 2\ln(\tfrac{1-\widetilde{g}_r(n)e^{\sqrt{\widetilde{\delta}_r(n)}\tau}}{1-\widetilde{g}_r(n)})],\\
&\widetilde{A}_4(\tau,n) = \tfrac{1-2\alpha}{2\alpha}\theta_1\widetilde{C}_1(\tau,n) + \tfrac{1-2\beta}{2\beta}\theta_2\widetilde{C}_2(\tau,n) + \tfrac{1-2\gamma}{2\gamma}\theta_r\widetilde{D}(\tau,n).\\
&a_0^*(n) = \lambda_0(E^{\mathbb{Q}}[e^{nJ_{01}}] - nm_{01} - 1) + \lambda_1(E^{\mathbb{Q}}[e^{nJ_{11}}] - nm_{11} - 1) - \tfrac{1}{2}L_0(f,f)(n-n^2)\\
&+\tfrac{1-2\alpha}{4\alpha}\theta_1 L_1(f,f)(n-n^2) + \tfrac{1-2\beta}{4\beta}\theta_2 L_2(f,f)(n-n^2) - \tfrac{1-2\gamma}{2\gamma}\theta_r(n-1),\\
&\widetilde{a}_1(n) = \tfrac{k_1\theta_1}{2\alpha} + \rho_{1v_1}(L_0(f,v_1^{\alpha}) + \tfrac{2\alpha-1}{2\alpha}L_1(f,v_1^{\alpha})\theta_1 + L_2(f,v_1^{\alpha})\theta_2)n,\\
&\widetilde{a}_2(n) = \tfrac{k_2\theta_2}{2\beta} + \rho_{1v_2}(L_0(f,v_2^{\beta}) + L_1(f,v_2^{\beta})\theta_1 + \tfrac{2\beta-1}{2\beta}L_2(f,v_2^{\beta})\theta_2)n.\\
&\widetilde{b}_1(n) = k_1 - \rho_{1v_1}L_1(f,v_1^{\alpha})n,\\
&\widetilde{b}_2(n) = k_2 - \rho_{1v_2}L_2(f,v_2^{\beta})n,\\
&\widetilde{b}_r(n) = k_r.\\
&\widetilde{c}_1(n) = -L_1(f,f)(n-n^2),\\
&\widetilde{c}_2(n) = -L_2(f,f)(n-n^2),\\
&\widetilde{c}_r(n) = 2(n-1).\\
&\widetilde{\delta}_1(n) = \widetilde{b}_1^2(n) - 2\alpha\sigma_1^2\theta_1^{2\alpha-1}\widetilde{c}_1(n),\\
&\widetilde{\delta}_2(n) = \widetilde{b}_2^2(n) - 2\beta\sigma_2^2\theta_2^{2\beta-1}\widetilde{c}_2(n),\\
&\widetilde{\delta}_r(n) = \widetilde{b}_r^2(n) - 2\gamma\sigma_r^2\theta_r^{2\gamma-1}\widetilde{c}_r(n).\\
&\widetilde{g}_1(n) = \tfrac{\widetilde{b}_1(n)+\sqrt{\widetilde{\delta}_1(n)}}{\widetilde{b}_1(n)-\sqrt{\widetilde{\delta}_1(n)}},\\
&\widetilde{g}_2(n) = \tfrac{\widetilde{b}_2(n)+\sqrt{\widetilde{\delta}_2(n)}}{\widetilde{b}_2(n)-\sqrt{\widetilde{\delta}_2(n)}},\\
&\widetilde{g}_r(n) = \tfrac{\widetilde{b}_r(n)+\sqrt{\widetilde{\delta}_r(n)}}{\widetilde{b}_r(n)-\sqrt{\widetilde{\delta}_r(n)}}.
\end{aligned}
$$

Proof. Refer to the first part of the Appendix for the specific proof. □

Lemma 2.2. *The boundedness of $M(t,T,y_1,v,r,n)$ depends on the boundedness of $e^{\widetilde{C}_1(\tau,n)v_1}$, $e^{\widetilde{C}_2(\tau,n)v_2}$, $e^{\widetilde{D}(\tau,n)r}$, and $e^{\widetilde{A}(\tau,n)}$. The terms $e^{\widetilde{C}_i(\tau,n)v_1}(i = 1,2)$ are bounded when one of the following conditions is satisfied:*

$$\begin{array}{ll}
(1) & \widetilde{\delta}_i(n) > 0, |\widetilde{b}_i(n)| < \sqrt{\widetilde{\delta}_i(n)}; \\
(2) & \widetilde{\delta}_i(n) > 0, \widetilde{b}_i(n) \geq \sqrt{\widetilde{\delta}_i(n)}; \\
(3) & \widetilde{\delta}_i(n) > 0, -\widetilde{b}_i(n) \geq \sqrt{\widetilde{\delta}_i(n)}, -\ln \widetilde{g}_i(n) \geq \sqrt{\widetilde{\delta}_i(n)}\tau; \\
(4) & \widetilde{\delta}_i(n) = 0, \widetilde{b}_i(n) \geq 0; \\
(5) & \widetilde{\delta}_i(n) = 0, \widetilde{b}_i(n) < 0, -\widetilde{b}_i(n)\tau < 2; \\
(6) & \widetilde{\delta}_i(n) < 0, \frac{\pi}{2} + \arctan \frac{\widetilde{b}_i(n)}{\sqrt{-\widetilde{\delta}_i(n)}} > \frac{\sqrt{-\widetilde{\delta}_i(n)}}{2}\tau.
\end{array} \tag{2.20}$$

The term $e^{\widetilde{D}(\tau,n)r}$ is bounded when one of the following conditions is satisfied:

$$\begin{array}{ll}
(1) & \widetilde{\delta}_r(n) > 0, \\
(2) & \widetilde{\delta}_r(n) = 0, -\widetilde{b}_r(n)\tau < 2; \\
(3) & \widetilde{\delta}_r(n) < 0, \frac{\pi}{2} + \arctan \frac{\widetilde{b}_r(n)}{\sqrt{-\widetilde{\delta}_r(n)}} > \frac{\sqrt{-\widetilde{\delta}_r(n)}}{2}\tau.
\end{array} \tag{2.21}$$

The term $e^{\widetilde{A}(\tau,n)}$ is bounded when the following condition is satisfied:

$$-\xi_1 < n < \eta_1. \tag{2.22}$$

Proof. Refer to the second part of the Appendix for the specific proof. □

It must be stated that the boundedness of $E^{\mathbb{Q}}[e^{-\int_t^T r_s ds} s_{1T}^{m-w} s_{1t^*} | \mathcal{F}_t]$ requires two guarantees. On the one side, $E^{\mathbb{Q}}[e^{-\int_{t^*}^T r_s ds} s_{1T}^{m-w} | \mathcal{F}_{t^*}]$ is finite, which gives the result

$$E^{\mathbb{Q}}[e^{-\int_t^T r_s ds} s_{1T}^{m-w} s_{1t^*}^{w} | \mathcal{F}_t] = E^{\mathbb{Q}}[e^{-\int_t^{t^*} r_s ds} s_{1t^*}^{m} | \mathcal{F}_t].$$

On the other side, $E^{\mathbb{Q}}[e^{-\int_t^{t^*} r_s ds} s_{1t^*}^{m} | \mathcal{F}_t]$ is also finite.

Lemma 2.3. *Let A, B, C, E be all constants, and $A \neq 0, B^2 - 4AC \neq 0$. Then the ordinary differential equations*

$$\begin{cases} \dfrac{\mathrm{d}y}{\mathrm{d}x} = Ay^2 + By + C, \\ y|_{x=0} = E, \end{cases}$$

have the solution that

$$y = \frac{y_1 - \frac{E-y_1}{E-y_2} y_2 \mathrm{e}^{dx}}{1 - \frac{E-y_1}{E-y_2}\mathrm{e}^{dx}} = \frac{(E-y_2)y_1 - (E-y_1)y_2\mathrm{e}^{dx}}{E - y_2 - (E-y_1)\mathrm{e}^{dx}},$$

where

$$d = \sqrt{B^2 - 4AC}, \quad y_1 = \frac{-B+d}{2A}, \quad y_2 = \frac{-B-d}{2A}.$$

Let $y_t = \ln(s_t) = (\ln s_{1t}, \ln s_{2t})$, $y = \ln(s) = (\ln s_1, \ln s_2)$, $u = (u_1, u_2, u_3, u_4, u_5)$. Then define the time t discounted conditional joint characteristic function of (y_T, v_T, r_T)

$$\begin{aligned} \varphi(t, T, y, v, r, u) &= E^{\mathbb{Q}}[e^{-\int_t^T r_s ds + iu_1 y_{1T} + iu_2 y_{2T} + iu_3 v_{1T} + iu_4 v_{2T} + iu_5 r_T} | \mathcal{F}_t] \\ &= E^{\mathbb{Q}}[e^{-\int_t^T r_s ds + iu_1 y_{1T} + iu_2 y_{2T} + iu_3 v_{1T} + iu_4 v_{2T} + iu_5 r_T} | y_t = y, v_t = v, r_t = r]. \end{aligned} \tag{2.23}$$

It should be noted that the expression $u = (u_1, u_2, u_3, u_4, u_5)$ is only valid within the characteristic function $\varphi(t, T, y, v, r, u)$.

Meanwhile, define the time t discounted conditional joint characteristic function of (y_T, v_T, y_{1t^*})

$$\begin{aligned} \Phi(t, T, t^*, y, v, r, u_1, u_2, u_3) &= E^{\mathbb{Q}}[e^{-\int_t^T r_s ds + iu_1 y_{1T} + iu_2 y_{2T} + iu_3 y_{1t^*}} | \mathcal{F}_t] \\ &= E^{\mathbb{Q}}[e^{-\int_t^T r_s ds + iu_1 y_{1T} + iu_2 y_{2T} + iu_3 y_{1t^*}} | y_t = y, v_t = v, r_t = r]. \end{aligned} \tag{2.24}$$

Consider that the essence of the risk-neutral pricing principle lies in converting the option price into probability calculations under different equivalent martingale measures, and that the joint characteristic function is a key technical and method for solving probability problems under multiple random factors. Facing the pricing problem of vulnerable powered options under the complex conditions of dual market volatility factors, interdependent jump structure, and random interest rates, the joint characteristic function method is a good choice. Moreover, because this problem involves asset prices at multiple moments and cannot solve the calculation of the characteristic function in one step, a phased backtracking method from far to near is adopted. Through martingale methods, by leveraging the natural martingale property of the conditional expectation of random variables, Theorem 2.4 first derives the joint characteristic function based on the future time point under various random factors. Furthermore, based on the accumulation property of the conditional expectation, the joint characteristic functions under the current moment are gradually resolved and computed in Theorem 2.5.

In the following, the approximate semi-analytical solutions of the two classes of characteristic functions are derived.

Theorem 2.4. *Suppose that the dynamics of process y_t is a general stochastic volatility process given by Eqs (2.1)–(2.5), and $\alpha, \beta, \gamma \in (0, 1]$, and the coefficients $f(v_1, v_2)$ and $g(v_1, v_2)$ satisfy the global Lipschitz condition and are square-integrable. The compound Poisson measure satisfies*

$$\int \min(1, |z|^2)\, \nu(dz) < \infty,$$

and the jump amplitudes satisfy the required integrability conditions. Then an approximate solution of $\varphi(t, T, y, v, r, u)$ is given by

$$e^{iu_1 y_1 + iu_2 y_2 + A(\tau,u) + (C_1(\tau,u) + iu_3) v_1 + (C_2(\tau,u) + iu_4) v_2 + (D(\tau,u) + iu_5) r}, \tag{2.25}$$

where $\tau = T - t$*,* $A(\tau, u)$*,* $C_1(\tau, u)$*,* $C_2(\tau, u)$*, and* $D(\tau, u)$ *are given by*

$$
\begin{aligned}
&A(\tau, u) = a_0(u)\tau + a_1(u)A_1(\tau, u) + a_2(u)A_2(\tau, u) + a_3(u)A_3(\tau, u) + A_4(\tau, u),\\
&C_1(\tau, u) = \tfrac{b_1(u)+\sqrt{\delta_1(u)}}{2\alpha\sigma_1^2\theta_1^{2\alpha-1}} \cdot \tfrac{1-e^{\sqrt{\delta_1(u)}\tau}}{1-g_1(u)e^{\sqrt{\delta_1(u)}\tau}}, C_2(\tau, u) = \tfrac{b_2(u)+\sqrt{\delta_2(u)}}{2\beta\sigma_2^2\theta_2^{2\beta-1}} \cdot \tfrac{1-e^{\sqrt{\delta_2(u)}\tau}}{1-g_2(u)e^{\sqrt{\delta_2(u)}\tau}},\\
&D(\tau, u) = \tfrac{b_r(u)+\sqrt{\delta_r(u)}}{2\gamma\sigma_r^2\theta_r^{2\gamma-1}} \cdot \tfrac{1-e^{\sqrt{\delta_r(u)}\tau}}{1-g_r(u)e^{\sqrt{\delta_r(u)}\tau}}.\\
&A_1(\tau, u) = \tfrac{1}{2\alpha\sigma_1^2\theta_1^{2\alpha-1}}[(b_1(u) + \sqrt{\delta_1(u)})\tau - 2\ln(\tfrac{1-g_1(u)e^{\sqrt{\delta_1(u)}\tau}}{1-g_1(u)})] + iu_3\tau,\\
&A_2(\tau, u) = \tfrac{1}{2\beta\sigma_2^2\theta_2^{2\beta-1}}[(b_2(u) + \sqrt{\delta_2(u)})\tau - 2\ln(\tfrac{1-g_2(u)e^{\sqrt{\delta_2(u)}\tau}}{1-g_2(u)})] + iu_4\tau,\\
&A_3(\tau, u) = \tfrac{1}{2\gamma\sigma_r^2\theta_r^{2\gamma-1}}[(b_r(u) + \sqrt{\delta_r(u)})\tau - 2\ln(\tfrac{1-g_r(u)e^{\sqrt{\delta_r(u)}\tau}}{1-g_r(u)})] + iu_5\tau,\\
&A_4(\tau, u) = \tfrac{1-2\alpha}{2\alpha}\theta_1 C_1(\tau, u) + \tfrac{1-2\beta}{2\beta}\theta_2 C_2(\tau, u) + \tfrac{1-2\gamma}{2\gamma}\theta_r D(\tau, u).\\
&a_0(u) = \lambda_0(E^{\mathbb{Q}}[e^{iu_1J_{01}+iu_2J_{02}}] - iu_1m_{01} - iu_2m_{02} - 1) + \lambda_1(E^{\mathbb{Q}}[e^{iu_1J_{11}}] - iu_1m_{11} - 1)\\
&+\lambda_2(E^{\mathbb{Q}}[e^{iu_2J_{12}}] - iu_2m_{12} - 1) - \tfrac{1}{2}L_0(f, f)(iu_1 + u_1^2) - \tfrac{1}{2}L_0(g, g)(iu_2 + u_2^2) - \rho_{12}L_0(f, g)u_1u_2\\
&+\tfrac{1-2\alpha}{2\alpha}\theta_1(\tfrac{1}{2}L_1(f, f)(iu_1 + u_1^2) + \tfrac{1}{2}L_1(g, g)(iu_2 + u_2^2) + \rho_{12}L_1(f, g)u_1u_2)\\
&+\tfrac{1-2\beta}{2\beta}\theta_2(\tfrac{1}{2}L_2(f, f)(iu_1 + u_1^2) + \tfrac{1}{2}L_2(g, g)(iu_2 + u_2^2) + \rho_{12}L_2(f, g)u_1u_2) - \tfrac{1-2\gamma}{2\gamma}\theta_r(iu_1 + iu_2 - 1),\\
&a_1(u) = \tfrac{k_1\theta_1}{2\alpha} + \rho_{1v_1}(L_0(f, v_1^\alpha) + \tfrac{2\alpha-1}{2\alpha}L_1(f, v_1^\alpha)\theta_1 + L_2(f, v_1^\alpha)\theta_2)iu_1\\
&+\rho_{2v_1}(L_0(g, v_1^\alpha) + \tfrac{2\alpha-1}{2\alpha}L_1(g, v_1^\alpha)\theta_1 + L_2(g, v_1^\alpha)\theta_2)iu_2,\\
&a_2(u) = \tfrac{k_2\theta_2}{2\beta} + \rho_{1v_2}(L_0(f, v_2^\beta) + L_1(f, v_2^\beta)\theta_1 + \tfrac{2\beta-1}{2\beta}L_2(f, v_2^\beta)\theta_2)iu_1\\
&+\rho_{2v_2}(L_0(g, v_2^\beta) + L_1(g, v_2^\beta)\theta_1 + \tfrac{2\beta-1}{2\beta}L_2(g, v_2^\beta)\theta_2)iu_2,\\
&a_3(u) = \tfrac{k_r\theta_r}{2\gamma}.\\
&b_1(u) = k_1 - \rho_{1v_1}L_1(f, v_1^\alpha)iu_1 - \rho_{2v_1}L_1(g, v_1^\alpha)iu_2 - 2\alpha\sigma_1^2\theta_1^{2\alpha-1}iu_3,\\
&b_2(u) = k_2 - \rho_{1v_2}L_2(f, v_2^\beta)iu_1 - \rho_{2v_2}L_1(g, v_2^\beta)iu_2 - 2\beta\sigma_2^2\theta_2^{2\beta-1}iu_4, b_r(u) = k_r - 2\gamma\sigma_r^2\theta_r^{2\gamma-1}iu_5.\\
&c_1(u) = -2(b_1(u) + \alpha\sigma_1^2\theta_1^{2\alpha-1}iu_3)iu_3 - L_1(f, f)(iu_1 + u_1^2) - L_1(g, g)(iu_2 + u_2^2) - 2\rho_{12}L_1(f, g)u_1u_2,\\
&c_2(u) = -2(b_2(u) + \beta\sigma_2^2\theta_2^{2\beta-1}iu_4)iu_4 - L_2(f, f)(iu_1 + u_1^2) - L_2(g, g)(iu_2 + u_2^2) - 2\rho_{12}L_2(f, g)u_1u_2,\\
&c_r(u) = -2(b_r(u) + \gamma\sigma_r^2\theta_r^{2\gamma-1}iu_5)iu_5 + 2(iu_1 + iu_2 - 1).\\
&\delta_1(u) = b_1^2(u) - 2\alpha\sigma_1^2\theta_1^{2\alpha-1}c_1(u), \delta_2(u) = b_2^2(u) - 2\beta\sigma_2^2\theta_2^{2\beta-1}c_2(u),\\
&\delta_r(u) = b_r^2(u) - 2\gamma\sigma_r^2\theta_r^{2\gamma-1}c_r(u), g_1(u) = \tfrac{b_1(u)+\sqrt{\delta_1(u)}}{b_1(u)-\sqrt{\delta_1(u)}}, g_2(u) = \tfrac{b_2(u)+\sqrt{\delta_2(u)}}{b_2(u)-\sqrt{\delta_2(u)}}, g_r(u) = \tfrac{b_r(u)+\sqrt{\delta_r(u)}}{b_r(u)-\sqrt{\delta_r(u)}}.\\
&L_1(f, g) = f_1'(\theta_1, \theta_2)g(\theta_1, \theta_2) + f(\theta_1, \theta_2)g_1'(\theta_1, \theta_2),\\
&L_2(f, g) = f_2'(\theta_1, \theta_2)g(\theta_1, \theta_2) + f(\theta_1, \theta_2)g_2'(\theta_1, \theta_2),\\
&L_0(f, g) = f(\theta_1, \theta_2)g(\theta_1, \theta_2) - L_1(f, g)\theta_1 - L_2(f, g)\theta_2.\\
&E^{\mathbb{Q}}[e^{iu_1J_{01}+iu_2J_{02}}] = e^{\mathbf{i}\mu_1u_1+\mathbf{i}\mu_2u_2-\frac{1}{2}(\sigma_{J_{01}}^2u_1^2+\sigma_{J_{02}}^2u_2^2+2\rho_{J_1J_2}\sigma_{J_{01}}\sigma_{J_{02}}u_1u_2)},\\
&E^{\mathbb{Q}}[e^{iu_1J_{11}}] = \tfrac{p_1\xi_1}{\xi_1+iu_1} + \tfrac{q_1\eta_1}{\eta_1-iu_1}, E^{\mathbb{Q}}[e^{iu_2J_{12}}] = \tfrac{p_2\xi_2}{\xi_2+iu_2} + \tfrac{q_2\eta_2}{\eta_2-iu_2}.
\end{aligned}
$$

Proof. According to Itô's lemma and the dynamics of two underlying assets, we have

$$
\begin{aligned}
dy_{1t} &= (r_t - \lambda_0 m_{01} - \lambda_1 m_{11} - \tfrac{1}{2}f^2(v_{1t}, v_{2t}))dt + f(v_{1t}, v_{2t})dW_{1t} + J_{01}dN_{0t} + J_{11}dN_{1t},\\
dy_{2t} &= (r_t - \lambda_0 m_{02} - \lambda_2 m_{12} - \tfrac{1}{2}g^2(v_{1t}, v_{2t}))dt + g(v_{1t}, v_{2t})dW_{2t} + J_{02}dN_{0t} + J_{12}dN_{2t}.
\end{aligned}
$$

From the Feynman–Kac formula, the option price $\varphi(t, T, y, v, r, u)$ satisfies a partial differential equation given by($\tau = T - t$):

$$
\begin{aligned}
&-\frac{\partial\varphi}{\partial\tau}+(r-\lambda_0 m_{01}-\lambda_1 m_{11}-\tfrac{1}{2}f^2(v_1,v_2))\frac{\partial\varphi}{\partial y_1}+(r-\lambda_0 m_{02}-\lambda_2 m_{12}-\tfrac{1}{2}g^2(v_1,v_2))\frac{\partial\varphi}{\partial y_2}\\
&+\tfrac{1}{2}f^2(v_1,v_2)\frac{\partial^2\varphi}{\partial y_1^2}+\tfrac{1}{2}g^2(v_1,v_2)\frac{\partial^2\varphi}{\partial y_2^2}+\rho_{12}f(v_1,v_2)g(v_1,v_2)\frac{\partial^2\varphi}{\partial y_1\partial y_2}+k_1(\theta_1-v_1)\frac{\partial\varphi}{\partial v_1}\\
&+k_2(\theta_2-v_2)\frac{\partial\varphi}{\partial v_2}+k_r(\theta_r-r)\frac{\partial\varphi}{\partial r}+\tfrac{1}{2}\sigma_1^2 v_1^{2\alpha}\frac{\partial^2\varphi}{\partial v_1^2}+\tfrac{1}{2}\sigma_2^2 v_2^{2\beta}\frac{\partial^2\varphi}{\partial v_2^2}+\tfrac{1}{2}\sigma_r^2 r^{2\gamma}\frac{\partial^2\varphi}{\partial r^2}\\
&+\rho_{1v_1}f(v_1,v_2)v_1^{\alpha}\frac{\partial^2\varphi}{\partial y_1\partial v_1}+\rho_{1v_2}f(v_1,v_2)v_2^{\beta}\frac{\partial^2\varphi}{\partial y_1\partial v_2}+\rho_{2v_1}g(v_1,v_2)v_1^{\alpha}\frac{\partial^2\varphi}{\partial y_2\partial v_1}\\
&+\rho_{2v_2}g(v_1,v_2)v_2^{\beta}\frac{\partial^2\varphi}{\partial y_2\partial v_2}-(r+\lambda_0+\lambda_1+\lambda_2)\varphi+\lambda_0 E^{\mathbb{Q}}[\varphi(t,T,y_1+J_{01},y_2+J_{02},v,r,u)]\\
&+\lambda_1 E^{\mathbb{Q}}[\varphi(t,T,y_1+J_{11},y_2,v,r,u)]+\lambda_2 E^{\mathbb{Q}}[\varphi(t,T,y_1,y_2+J_{12},v_1,v_2,r,u)]=0
\end{aligned}
$$

with the boundary condition $\varphi(T,T,y,v,r,u)=e^{iu_1y_1+iu_2y_2+iu_3v_1+iu_4v_2+iu_5r}$.

Drawing on the research approach of the referenced literature [30], by the technique of total differentiation of multivariate functions, apply the first-order Taylor approximation to the long-term mean (θ_1,θ_2) to derive

$$
\begin{aligned}
&f(v_1,v_2)g(v_1,v_2)\\
\approx\ & f(\theta_1,\theta_2)g(\theta_1,\theta_2)+\frac{\partial f(v_1,v_2)g(v_1,v_2)}{\partial v_1}|_{(\theta_1,\theta_2)}(v_1-\theta_1)+\frac{\partial f(v_1,v_2)g(v_1,v_2)}{\partial v_2}|_{(\theta_1,\theta_2)}(v_2-\theta_2)\\
=\ & L_0(f,g)+L_1(f,g)v_1+L_2(f,g)v_2
\end{aligned}
$$

with the core coefficient

$$
\begin{aligned}
L_1(f,g) &= \frac{\partial f(v_1,v_2)g(v_1,v_2)}{\partial v_1}|_{(\theta_1,\theta_2)}=f_1'(\theta_1,\theta_2)g(\theta_1,\theta_2)+f(\theta_1,\theta_2)g_1'(\theta_1,\theta_2),\\
L_2(f,g) &= \frac{\partial f(v_1,v_2)g(v_1,v_2)}{\partial v_2}|_{(\theta_1,\theta_2)}=f_2'(\theta_1,\theta_2)g(\theta_1,\theta_2)+f(\theta_1,\theta_2)g_2'(\theta_1,\theta_2),\\
L_0(f,g) &= f(\theta_1,\theta_2)g(\theta_1,\theta_2)-L_1(f,g)\theta_1-L_2(f,g)\theta_2.
\end{aligned}
$$

Substituting the above nonlinear PDE, the following approximate linear PDE can be derived:

$$
\begin{aligned}
&-\frac{\partial\varphi}{\partial\tau}+[r-\lambda_0 m_{01}-\lambda_1 m_{11}-\tfrac{1}{2}L_0(f,f)-\tfrac{1}{2}L_1(f,f)v_1-\tfrac{1}{2}L_2(f,f)v_2]\frac{\partial\varphi}{\partial y_1}\\
&+[r-\lambda_0 m_{02}-\lambda_2 m_{12}-\tfrac{1}{2}L_0(g,g)-\tfrac{1}{2}L_1(g,g)v_1-\tfrac{1}{2}L_2(g,g)v_2]\frac{\partial\varphi}{\partial y_2}\\
&+\tfrac{1}{2}[L_0(f,f)+L_1(f,f)v_1+L_2(f,f)v_2]\frac{\partial^2\varphi}{\partial y_1^2}+\tfrac{1}{2}[L_0(g,g)+L_1(g,g)v_1+L_2(g,g)v_2]\frac{\partial^2\varphi}{\partial y_2^2}\\
&+\rho_{12}[L_0(f,g)+L_1(f,g)v_1+L_2(f,g)v_2]\frac{\partial\varphi}{\partial y_1\partial y_2}+k_1(\theta_1-v_1)\frac{\partial\varphi}{\partial v_1}+k_2(\theta_2-v_2)\frac{\partial\varphi}{\partial v_2}\\
&+k_r(\theta_r-r)\frac{\partial\varphi}{\partial r}+\tfrac{1}{2}\sigma_1^2[(1-2\alpha)\theta_1^{2\alpha}+2\alpha\theta_1^{2\alpha-1}v_1]\frac{\partial^2\varphi}{\partial v_1^2}\\
&+\tfrac{1}{2}\sigma_2^2[(1-2\beta)\theta_2^{2\beta}+2\beta\theta_2^{2\beta-1}v_2]\frac{\partial^2\varphi}{\partial v_2^2}+\tfrac{1}{2}\sigma_r^2[(1-2\gamma)\theta_r^{2\gamma}+2\gamma\theta_r^{2\gamma-1}r]\frac{\partial^2\varphi}{\partial r^2}\\
&+\rho_{1v_1}[L_0(f,v_1^{\alpha})+L_1(f,v_1^{\alpha})v_1+L_2(f,v_1^{\alpha})v_2]\frac{\partial^2\varphi}{\partial y_1\partial v_1}\\
&+\rho_{1v_2}[L_0(f,v_1^{\beta})+L_1(f,v_2^{\beta})v_1+L_2(f,v_2^{\beta})v_2]\frac{\partial^2\varphi}{\partial y_1\partial v_2}\\
&+\rho_{2v_1}[L_0(g,v_1^{\alpha})+L_1(g,v_1^{\alpha})v_1+L_2(g,v_1^{\alpha})v_2]\frac{\partial^2\varphi}{\partial y_2\partial v_1}\\
&+\rho_{2v_2}[L_0(g,v_1^{\beta})+L_1(g,v_2^{\beta})v_1+L_2(g,v_2^{\beta})v_2]\frac{\partial^2\varphi}{\partial y_2\partial v_2}\\
&+\lambda_0 E^{\mathbb{Q}}[\varphi(t,T,y_1+J_{01},y_2+J_{02},v,r,u)]+\lambda_1 E^{\mathbb{Q}}[\varphi(t,T,y_1+J_{11},y_2,v,r,u)]\\
&+\lambda_2 E^{\mathbb{Q}}[\varphi(t,T,y_1,y_2+J_{12},v,r,u)]-(r+\lambda_0+\lambda_1+\lambda_2)\varphi=0
\end{aligned}
$$

with the boundary condition $\varphi(T,T,y,v,r,u)=e^{iu_1y_1+iu_2y_2+iu_3v_1+iu_4v_2+iu_5r}$.

Assume that $\varphi(t,T,y,v,r,u)$ is of the form

$$
\varphi(t,T,y,v,r,u)=e^{iu_1y_1+iu_2y_2+A(\tau,u)+(C_1(\tau,u)+iu_3)v_1+(C_2(\tau,u)+iu_4)v_2+(D(\tau,u)+iu_5)r}.
$$

Then, we obtain

$$E^{\mathbb{Q}}[\varphi(t,T,y_1+J_{11},y_2,v,r,u)]=\varphi(t,T,y_1,y_2,v,r,u)E^{\mathbb{Q}}[e^{iu_1J_{11}}],$$
$$E^{\mathbb{Q}}[\varphi(t,T,y_1,y_{12}+J_{12},v,r,u)]=\varphi(t,T,y_1,y_2,v,r,u)E^{\mathbb{Q}}[e^{iu_2J_{12}}],$$
$$E^{\mathbb{Q}}[\varphi(t,T,y_1+J_{01},y_2+J_{02},v,r,u)]=\varphi(t,T,y_1,y_2,v,r,u)E^{\mathbb{Q}}[e^{iu_1J_{01}+iu_2J_{02}}].$$

Further, $A(\tau,u)$, $C_1(\tau,u)$,$C_2(\tau,u)$, and $D(\tau,u)$ become solutions of Riccati differential equations:

$$\begin{aligned}
&\tfrac{\partial A}{\partial\tau}=\lambda_0(E^{\mathbb{Q}}[e^{iu_1J_{01}+iu_2J_{02}}]-iu_1m_{01}-iu_2m_{02}-1)+\lambda_1(E^{\mathbb{Q}}[e^{iu_1J_{11}}]-iu_1m_{11}-1)\\
&+\lambda_2(E^{\mathbb{Q}}[e^{iu_2J_{12}}]-iu_2m_{12}-1)-\tfrac{1}{2}L_0(f,f)(iu_1+u_1^2)-\tfrac{1}{2}L_0(g,g)(iu_2+u_2^2)-\rho_{12}L_0(f,g)u_1u_2\\
&+[k_1\theta_1+\rho_{1v_1}(L_0(f,v_1^{\alpha})+L_2(f,v_1^{\alpha})\theta_2)iu_1+\rho_{2v_1}(L_0(g,v_1^{\alpha})+L_2(g,v_1^{\alpha})\theta_2)iu_2](C_1+iu_3)\\
&+[k_2\theta_2+\rho_{1v_2}(L_0(f,v_2^{\beta})+L_1(f,v_2^{\beta})\theta_1)iu_1+\rho_{2v_2}(L_0(g,v_2^{\beta})+L_1(g,v_2^{\beta})\theta_1)iu_2](C_2+iu_4)\\
&+k_r\theta_r(D+iu_5)+\tfrac{1}{2}(1-2\alpha)\sigma_1^2\theta_1^{2\alpha}(C_1+iu_3)^2+\tfrac{1}{2}(1-2\beta)\sigma_2^2\theta_2^{2\beta}(C_2+iu_4)^2+\tfrac{1}{2}(1-2\gamma)\sigma_r^2\theta_r^{2\gamma}(D+iu_5)^2,\\
&\tfrac{\partial C_1}{\partial\tau}=\alpha\sigma_1^2\theta_1^{2\alpha-1}(C_1+iu_3)^2-(k_1-\rho_{1v_1}L_1(f,v_1^{\alpha})iu_1-\rho_{2v_1}L_1(g,v_1^{\alpha})iu_2)(C_1+iu_3)\\
&-\tfrac{1}{2}L_1(f,f)(iu_1+u_1^2)-\tfrac{1}{2}L_1(g,g)(iu_2+u_2^2)-\rho_{12}L_1(f,g)u_1u_2,\\
&\tfrac{\partial C_2}{\partial\tau}=\beta\sigma_2^2\theta_2^{2\beta-1}(C_2+iu_4)^2-(k_2-\rho_{1v_2}L_2(f,v_2^{\beta})iu_1-\rho_{2v_2}L_2(g,v_2^{\beta})iu_2)(C_2+iu_4)\\
&-\tfrac{1}{2}L_2(f,f)(iu_1+u_1^2)-\tfrac{1}{2}L_2(g,g)(iu_2+u_2^2)-\rho_{12}L_2(f,g)u_1u_2,\\
&\tfrac{\partial D}{\partial\tau}=\gamma\sigma_r^2\theta_r^{2\gamma-1}(D+iu_5)^2-k_r(D+iu_5)+iu_1+iu_2-1,
\end{aligned}$$

with the boundary condition $A(0,u)=0,C_1(0,u)=0,C_2(0,u)=0,D(0,u)=0$.

Obviously, the above system of equations is the Riccati system of equations. By applying Lemma 2.3, an analytical formula $C_1(\tau,u)$, $C_2(\tau,u)$, and $D(\tau,u)$ can be easily obtained. Furthermore, substitute it into the equation that $A(\tau,u)$ satisfies and then integrate term by term to obtain the analytical formula of $A(\tau,u)$. □

Remark 1. The above theorem provides the approximate formula derived through the linearization method under the condition α,$\beta,\gamma\in(0,1]$. Below, the processing method under the given condition $\alpha=0$ or $\beta=0$ or $\gamma=0$ is presented. Next, taking the interest rate r_t or $\gamma=0$ as an example, the general processing approach for such problems is illustrated. First, when $\gamma=0$, then there is

$$dr_t=k_r(\theta_r-r_t)dt+\sigma_r dW_{rt}.$$

Therefore, in this paper, we assume that the interest rate model degenerates into the observed Hull–White model. Second, under the condition that other factors remain unchanged, the equation which $D(\tau,u)$ satisfies transforms into

$$\frac{\partial D}{\partial\tau}=-k_r(D+iu_5)+iu_1+iu_2-1,D(0,u)=0.$$

Because the above equation is a first-order nonhomogeneous linear differential equation, the formula can be immediately obtained as

$$D(\tau,u)=\frac{c_r(u)}{b_r(u)}(1-e^{-b_r(u)\tau}).$$

Finally, replace all the occurrences of $D(\tau,u)$ with this formula, and we will obtain all the results. When $\alpha=0$, or $\beta=0$, $C_1(\tau,u)$ and $C_2(\tau,u)$ can be handled in a similar way.

Theorem 2.5. *Suppose that the dynamics of process y_t is an general stochastic volatility process given by Eqs (2.1)–(2.5). Then an approximate solution to $\Phi(t, T, t^*, y, v, r, u_1, u_2, u_3)$ is given by*

$$e^{A(\tau_1,\bar{u})} \cdot \varphi(t, t^*, y, v, r, u_1 + u_3, u_2, -iC_1(\tau_1, \bar{u}), -iC_2(\tau_1, \bar{u}), -iD(\tau_1, \bar{u})), \tag{2.26}$$

where $\tau = T - t, \tau_1 = T - t^*, \tau_2 = t^* - t, \bar{u} = (u_1, u_2, 0, 0, 0)$.

Proof. Let $\tau = T - t, \tau_1 = T - t^*, \tau_2 = t^* - t, \bar{u} = (u_1, u_2, 0, 0, 0)$. From the cumulative property of conditional expectation and the conclusion of the theorem above, it can be straightfowardly obtained that

$$\begin{aligned}
&\Phi(t, T, t^*, y, v, r, u_1, u_2, u_3) = E^{\mathbb{Q}}[e^{-\int_t^T r_s ds + iu_1 y_{1T} + iu_2 y_{2T} + iu_3 y_{1t^*}} | \mathcal{F}_t] \\
= \ & E^{\mathbb{Q}}[E^{\mathbb{Q}}[e^{-\int_t^T r_s ds + iu_1 y_{1T} + iu_2 y_{2T} + iu_3 y_{1t^*}} | \mathcal{F}_{t^*}] | \mathcal{F}_t] \\
= \ & E^{\mathbb{Q}}[e^{-\int_t^{t^*} r_s ds + iu_3 y_{1t^*}} E^{\mathbb{Q}}[e^{-\int_{t^*}^T r_s ds + iu_1 y_{1T} + iu_2 y_{2T}} | \mathcal{F}_{t^*}] | \mathcal{F}_t]
\end{aligned}$$

From the knowledge of stochastic analysis, it can be known that the Itô process satisfies the Markov property. Also v_{1t}, v_{2t}, and r_t are standard Itô processes, so v_{1t}, v_{2t}, and r_t all satisfy the Markov property. Considering that y_{1t} and y_{2t} can all be decomposed into the sum of independent Itô processes and compound Poisson processes, and because the compound Poisson process satisfies the property of independent increments, according to the independence lemma, it can be concluded that y_{1t} and y_{2t} still have the Markov property. Because the characteristic function $\varphi(t, T, y, v, r, u)$ only contains five random factors $(y_{1T}, y_{2T}, v_{1T}, v_{2T}, r_T)$, and given its Markov property along with the definition of the characteristic function $\varphi(t, T, y, v, r, u)$, we can obtain ($\tau_1 = T - t^*$)

$$\begin{aligned}
& E^{\mathbb{Q}}[e^{-\int_{t^*}^T r_s ds + iu_1 y_{1T} + iu_2 y_{2T}} | \mathcal{F}_{t^*}] \\
= \ & \varphi(t^*, T, y_{t^*}, v_{t^*}, r_{t^*}, \bar{u}) \\
= \ & e^{iu_1 y_{1t^*} + iu_2 y_{2t^*} + A(\tau_1,\bar{u}) + C_1(\tau_1,\bar{u}) v_{1t^*} + C_2(\tau_1,\bar{u}) v_{2t^*} + D(\tau_1,\bar{u}) r_{t^*}}.
\end{aligned}$$

Substituting the above formula and further simplifying, we obtain

$$\begin{aligned}
& \Phi(t, T, t^*, y, v, r, u_1, u_2, u_3) \\
= \ & E^{\mathbb{Q}}[e^{-\int_t^{t^*} r_s ds + iu_3 y_{1t^*}} \cdot e^{iu_1 y_{1t^*} + iu_2 y_{2t^*} + A(\tau_1,\bar{u}) + C_1(\tau_1,\bar{u}) v_{1t^*} + C_2(\tau_1,\bar{u}) v_{2t^*} + D(\tau_1,\bar{u}) r_{t^*}} | \mathcal{F}_t] \\
= \ & E^{\mathbb{Q}}[e^{-\int_t^{t^*} r_s ds + (iu_1 + iu_3) y_{1t^*} + iu_2 y_{2t^*} + A(\tau_1,\bar{u}) + C_1(\tau_1,\bar{u}) v_{1t^*} + C_2(\tau_1,\bar{u}) v_{2t^*} + D(\tau_1,\bar{u}) r_{t^*}} | \mathcal{F}_t].
\end{aligned}$$

Finally, let $u = (u_1 + u_3, u_2, -iC_1(\tau_1, \bar{u}), -iC_2(\tau_1, \bar{u}), -iD(\tau_1, \bar{u}))$, generate a new characteristic function, and we can obtain

$$\begin{aligned}
& \Phi(t, T, t^*, y, v, r, u_1, u_2, u_3) \\
= \ & e^{A(\tau_1,\bar{u})} \cdot \varphi(t, t^*, y, v, r, u_1 + u_3, u_2, -iC_1(\tau_1, \bar{u}), -iC_2(\tau_1, \bar{u}), -iD(\tau_1, \bar{u})).
\end{aligned}$$

□

3. Pricing V_1 and V_2

In this section, we treat V_1 and V_2 as two new types of vulnerable options with parameter w. Applying a measure transform and characteristic function, the semi-analytical closed solutions of V_1

and V_2 are finally obtained in integral form. In the investment of options, the risk hedging share plays a very important role. Therefore, the following presents the definition of the risk hedging share (delta) Δ_1 and Δ_2 of the underlying asset s_{1t} regarding V_1 and V_2, and the calculation formula is given in the subsequent theorem. Specifically,

$$\triangle_1(t,T,m,w|s,v,r)=\frac{\partial V_1(t,T,m,w|s,v,r)}{\partial s_1},\triangle_2(t,T,m,w|s,v,r)=\frac{\partial V_2(t,T,m,w|s,v,r)}{\partial s_1}.$$

Theorem 3.1. *The price and delta at time $t\in[0,T]$ of $V_1(t,T,m,w|s,v,r)$ under the above proposed model (2.1)–(2.5) are given by*

$$\begin{aligned}
& V_1(t,T,m,w|s,v,r)\\
= \ & \varphi(t,T,y,v,r,-i(m-w),0,0,0,0)F(\ln D^*,\varphi_1(0,u))\\
& +\tfrac{(1-\varpi)}{D}\varphi(t,T,y,v,r,-i(m-w),-i,0,0,0)F(-\ln D^*,\varphi_2(0,-u)),\\
& \triangle_1(t,T,m,w|s,v,r)\\
= \ & (m-w)\varphi(t,T,y,v,r,-i(m-w),0,0,0,0)\cdot e^{-y_1}\cdot F(\ln D^*,\varphi_1(0,u))\\
& +\tfrac{(1-\varpi)}{D}(m-w)\varphi(t,T,y,v,r,-i(m-w),-i,0,0,0)\cdot e^{-y_1}\cdot F(-\ln D^*,\varphi_2(0,-u))],
\end{aligned} \tag{3.1}$$

where

$$\begin{aligned}
\varphi_1(u_1,u_2)&=\frac{\varphi(t,T,y,v,r,u_1-i(m-w),u_2,0,0,0)}{\varphi(t,T,y,v,r,-i(m-w),0,0,0,0)},\\
\varphi_2(u_1,u_2)&=\frac{\varphi(t,T,y,v,r,u_1-i(m-w),u_2-i,0,0,0)}{\varphi(t,T,y,v,r,-i(m-w),-i,0,0,0)},\\
F(a,\phi(u))&=\frac{1}{2}+\frac{1}{\pi}\int_0^{+\infty}Re[\frac{e^{-iua}\phi(u)}{iu}]du.
\end{aligned}$$

Proof. According to the principle of risk-neutral pricing and the payoff at the maturity time T, we have

$$\begin{aligned}
& V_1(t,T,m,w|s,v,r)\\
= \ & E^{\mathbb{Q}}[e^{-\int_t^T r_s ds}s_{1T}^{m-w}(1_{\{s_{2T}\geq D^*\}}+\tfrac{1-\varpi}{D}s_{2T}1_{\{s_{2T}<D^*\}})|\mathcal{F}_t]\\
= \ & E^{\mathbb{Q}}[e^{-\int_t^T r_s ds}s_{1T}^{m-w}1_{\{s_{2T}\geq D^*\}}|\mathcal{F}_t]+\tfrac{(1-\varpi)}{D}E^{\mathbb{Q}}[e^{-\int_t^T r_s ds}s_{1T}^{m-w}s_{2T}1_{\{s_{2T}<D^*\}}|\mathcal{F}_t].
\end{aligned}$$

In order to further calculate, it is necessary to define the new equivalent martingale measures P_1 and P_2 of the risk-neutral measure. The Radon–Nikodym derivatives are established by

$$\begin{aligned}
\frac{dP_1}{dQ} &= \frac{e^{-\int_t^T r_s ds}s_{1T}^{m-w}}{\varphi(t,T,y,v,r,-i(m-w),0,0,0,0)},\\
\frac{dP_2}{dQ} &= \frac{e^{-\int_t^T r_s ds}s_{1T}^{m-w}S_{2T}}{\varphi(t,T,y,v,r,-i(m-w),-i,0,0,0)}.
\end{aligned}$$

Furthermore, the above two expressions for the derivative P_1 and P_2 of Radon–Nikodym satisfy the conditions for measure transformation.

First, the numerator $e^{-\int_t^T r_s ds}s_{1T}^{m-w}>0$ is obviously true, and based on the definition of the characteristic function $\varphi(t,T,y,v,r,u)$, the denominator becomes $\varphi(t,T,y,v,r,-i(m-w),-i,0,0,0)=E^{\mathbb{Q}}[e^{-\int_t^T r_s ds}s_{1T}^{m-w}|\mathcal{F}_t]>0$; that is, $\frac{dP_1}{dQ}>0$.

Second, explain the martingale property of $\frac{dP_1}{dQ}$. For the convenience of verification, by generating the process $\frac{dP_1}{dQ}|_{t_1}$of calculating the derivative of $\frac{dP_1}{dQ}$, we can obtain ($t \le t_1 \le T$)

$$\frac{dP_1}{dQ}|_{t_1} = E^{\mathbb{Q}}[\frac{e^{-\int_t^T r_s ds} s_{1T}^{m-w}}{E^{\mathbb{Q}}[e^{-\int_t^T r_s ds} s_{1T}^{m-w}|\mathcal{F}_t]}|\mathcal{F}_{t_1}] = \frac{E^{\mathbb{Q}}[e^{-\int_t^T r_s ds} s_{1T}^{m-w}|\mathcal{F}_{t_1}]}{E^{\mathbb{Q}}[e^{-\int_t^T r_s ds} s_{1T}^{m-w}|\mathcal{F}_t]}.$$

Under the condition $t \le t_1 \le t_2 \le T$ and the cumulative nature of the conditional expectation, it can be dirived that

$$E^{\mathbb{Q}}[\frac{dP_1}{dQ}|_{t_2}|\mathcal{F}_{t_1}] = E^{\mathbb{Q}}[\frac{e^{-\int_t^T r_s ds} s_{1T}^{m-w}}{E^{\mathbb{Q}}[e^{-\int_t^T r_s ds} s_{1T}^{m-w}|\mathcal{F}_t]}|\mathcal{F}_{t_2}|\mathcal{F}_{t_1}] = \frac{E^{\mathbb{Q}}[e^{-\int_t^T r_s ds} s_{1T}^{m-w}|\mathcal{F}_{t_1}]}{E^{\mathbb{Q}}[e^{-\int_t^T r_s ds} s_{1T}^{m-w}|\mathcal{F}_t]} = \frac{dP_1}{dQ}|_{t_1}.$$

Third, we verify the absolute integrability of $\frac{dP_1}{dQ}$. On the one hand, Lemma 2.2 provides the specific approximate conditions for its integrability (let $n = m - Re(w)$), which will not be elaborated upon here. On the other hand, according to the following formula,

$$E^{\mathbb{Q}}[\frac{dP_1}{dQ}|\mathcal{F}_t] = E^{\mathbb{Q}}[\frac{e^{-\int_t^T r_s ds} s_{1T}^{m-w}}{E^{\mathbb{Q}}[e^{-\int_t^T r_s ds} s_{1T}^{m-w}|\mathcal{F}_t]}|\mathcal{F}_t] = \frac{E^{\mathbb{Q}}[e^{-\int_t^T r_s ds} s_{1T}^{m-w}|\mathcal{F}_t]}{E^{\mathbb{Q}}[e^{-\int_t^T r_s ds} s_{1T}^{m-w}|\mathcal{F}_t]} = 1,$$

$E^{\mathbb{Q}}[\frac{dP_1}{dQ}|\mathcal{F}_t] = 1$ can be obtained. The situation of P_2 can be verified through similar reasoning.

Next, define the joint characteristic functions of (y_{1T}, y_{2T}) under the new measure P_1 and P_2,

$$\varphi_1(u_1, u_2) = E^{\mathbb{P}_1}[e^{iu_1 y_{1T} + iu_2 y_{2T}}|\mathcal{F}_t],$$

$$\varphi_2(u_1, u_2) = E^{\mathbb{P}_2}[e^{iu_1 y_{1T} + iu_2 y_{2T}}|\mathcal{F}_t],$$

where (u_1, u_2) represent coefficient variations of (y_{1T}, y_{2T}).

The new joint characteristic functions under the new probability measures P_1, P_2 are given by

$$\begin{aligned}
\varphi_1(u_1, u_2) = \quad & E^{\mathbb{Q}}[\frac{e^{-\int_t^T r_s ds + ((m-w)+iu_1)y_{1T} + iu_2 y_{2T}}}{\varphi(t,T,y,v,r,-i(m-w),0,0,0,0)}|\mathcal{F}_t] = \frac{\varphi(t,T,y,v,r,u_1-i(m-w),u_2,0,0,0)}{\varphi(t,T,y,v,r,-i(m-w),0,0,0,0)}, \\
\varphi_2(u_1, u_2) = \quad & E^{\mathbb{Q}}[\frac{e^{-\int_t^T r_s ds + ((m-w)+iu_1)y_{1T} + (1+iu_2)y_{2T}}}{\varphi(t,T,y,v,r,-i(m-w),-i,0,0,0)}|\mathcal{F}_t] = \frac{\varphi(t,T,y,v,r,u_1-i(m-w),u_2-i,0,0,0)}{\varphi(t,T,y,v,r,-i(m-w),-i,0,0,0)}.
\end{aligned}$$

Further, by applying the joint characteristic functions $\varphi_1(u_1, u_2)$, $\varphi_2(u_1, u_2)$, we obtain the final result

$$\begin{aligned}
& V_1(t, T, m, w|s, v, r) \\
= \quad & \varphi(t, T, y, v, r, -i(m-w), 0, 0, 0, 0)E^{\mathbb{P}_1}[1_{\{s_{2T} \ge D^*\}}|\mathcal{F}_t] \\
& + \tfrac{(1-\varpi)}{D}\varphi(t, T, y, v, r, -i(m-w), -i, 0, 0, 0)E^{\mathbb{P}_2}[1_{\{s_{2T} < D^*\}}|\mathcal{F}_t], \\
= \quad & \varphi(t, T, y, v, r, -i(m-w), 0, 0, 0, 0)P_1\{y_{2T} \ge \ln D^*|\mathcal{F}_t\} \\
& + \tfrac{(1-\varpi)}{D}\varphi(t, T, y, v, r, -i(m-w), -i, 0, 0, 0)P_2\{y_{2T} < \ln D^*|\mathcal{F}_t\} \\
= \quad & \varphi(t, T, y, v, r, -i(m-w), 0, 0, 0, 0)F(\ln D^*, \varphi_1(0, u)) \\
& + \tfrac{(1-\varpi)}{D}\varphi(t, T, y, v, r, -i(m-w), -i, 0, 0, 0)F(-\ln D^*, \varphi_2(0, -u)).
\end{aligned}$$

In a similar line to $\triangle_1(t, T, m, w|s, v, r)$, we can obtain ($y_1 = \ln(s_1)$):

$$\triangle_1(t, T, m, w|s, v, r) = \frac{\partial V_1(t,T,m,w|s,v,r)}{\partial s_1} = \frac{\partial V_1(t,T,m,w|s,v,r)}{\partial y_1} \cdot \frac{1}{s_1} = \frac{\partial V_1(t,T,m,w|s,v,r)}{\partial y_1} \cdot e^{-y_1}.$$

According to the expression of $\varphi(t, T, y, v, r, u)$ in Theorem 2.4, we can obtain

$$\frac{\partial \varphi(t, T, y, v, r, -i(m-w), 0, 0, 0, 0)}{\partial y_1} = (m-w)\varphi(t, T, y, v, r, -i(m-w), 0, 0, 0, 0),$$
$$\frac{\partial \varphi(t, T, y, v, r, -i(m-w), -i, 0, 0, 0)}{\partial y_1} = (m-w)\varphi(t, T, y, v, r, -i(m-w), -i, 0, 0, 0).$$

From the expression of $\varphi_1(u_1, u_2)$ and $\varphi_2(u_1, u_2)$, it can be further known that $\varphi_1(0, u)$ and $\varphi_2(0, -u)$ do not contain variable y_1. Therefore, the following facts hold true:

$$\frac{\partial F(\ln D^*, \varphi_1(0, u))}{\partial y_1} = \frac{\partial F(-\ln D^*, \varphi_2(0, -u))}{\partial y_1} = 0.$$

Continue to differentiate and substitute the above conclusion; then, we can obtain the final result.

$$\begin{aligned} & \triangle_1(t, T, m, w|s, v, r) \\ = \; & (m-w)\varphi(t, T, y, v, r, -i(m-w), 0, 0, 0, 0) \cdot e^{-y_1} \cdot F(\ln D^*, \varphi_1(0, u)) \\ & + \tfrac{(1-\varpi)}{D}(m-w)\varphi(t, T, y, v, r, -i(m-w), -i, 0, 0, 0) \cdot e^{-y_1} \cdot F(-\ln D^*, \varphi_2(0, -u)). \end{aligned}$$

□

Theorem 3.2. *The price and delta at time $t \in [0, T]$ of $V_2(t, T, m, w|s, v, r)$ under the above proposed model (2.1)–(2.5), are given by*

$$\begin{aligned} & V_2(t, T, m, w|s, v, r) \\ = \; & \Phi(t, T, t^*, y, v, r, -i(m-w), 0, -iw)F(\ln D^*, \varphi_3(0, u, 0)) \\ & + \tfrac{(1-\varpi)}{D}\Phi(t, T, t^*, y, v, r, -i(m-w), -i, -iw)F(-\ln D^*, \varphi_4(0, -u, 0)), \\ & \triangle_2(t, T, m, w|s, v, r) \\ = \; & m\Phi(t, T, t^*, y, v, r, -i(m-w), 0, -iw) \cdot e^{-y_1} \cdot F(\ln D^*, \varphi_3(0, u, 0)) \\ & + \tfrac{(1-\varpi)}{D}m\Phi(t, T, t^*, y, v, r, -i(m-w), -i, -iw) \cdot e^{-y_1} \cdot F(-\ln D^*, \varphi_4(0, -u, 0)), \end{aligned} \tag{3.2}$$

where $\varphi_3(u_1, u_2, u_3) = \frac{\Phi(t,T,t^*,y,v,r,u_1-i(m-w),u_2,u_3-iw)}{\Phi(t,T,t^*,y,v,r,-i(m-w),0,-iw)}$,
$\varphi_4(u_1, u_2, u_3) = \frac{\Phi(t,T,t^*,y,v,r,u_1-i(m-w),u_2-i,u_3-iw)}{\Phi(t,T,t^*,y,v,r,-i(m-w),-i,-iw)}$.

Proof. According to the principle of risk-neutral pricing and the payoff at the maturity time T, we have

$$\begin{aligned} & V_2(t, T, m, w|s, v, r) \\ = \; & E^{\mathbb{Q}}[e^{-\int_t^T r_s ds} s_{1T}^{m-w} s_{1t^*}^{w} (1_{\{s_{2T} \geq D^*\}} + \tfrac{1-\varpi}{D} s_{2T} 1_{\{s_{2T} < D^*\}})|\mathcal{F}_t] \\ = \; & E^{\mathbb{Q}}[e^{-\int_t^T r_s ds} s_{1T}^{m-w} s_{1t^*}^{w} 1_{\{s_{2T} \geq D^*\}}|\mathcal{F}_t] + \tfrac{(1-\varpi)}{D} E^{\mathbb{Q}}[e^{-\int_t^T r_s ds} s_{1T}^{m-w} s_{1t^*}^{w} s_{2T} 1_{\{s_{2T} < D^*\}}|\mathcal{F}_t]. \end{aligned}$$

By applying the joint characteristic functions $\Phi(t, T, t^*, y, v, r, u)$, we obtain the result

$$\begin{aligned} & V_2(t, T, m, w|s, v, r) \\ = \; & \Phi(t, T, t^*, y, v, r, -i(m-w), 0, 0)E^{\mathbb{P}_1}[s_{1t^*}^{w} 1_{\{s_{2T} \geq D^*\}}|\mathcal{F}_t] \\ & + \tfrac{(1-\varpi)}{D}\Phi(t, T, t^*, y, v, r, -i(m-w), -i, 0)E^{\mathbb{P}_2}[s_{1t^*}^{w} 1_{\{s_{2T} < D^*\}}|\mathcal{F}_t]. \end{aligned}$$

In order to further calculate, it is necessary to define the new equivalent martingale measures P_3, P_4 of the risk-neutral measure. The Radon–Nikodym derivatives are established by

$$\tfrac{dP_3}{dP_1} = \frac{s_{1t^*}^{w}}{E^{\mathbb{P}_1}[s_{1t^*}^{w}|\mathcal{F}_t]}, \tfrac{dP_4}{dP_2} = \frac{s_{1t^*}^{w}}{E^{\mathbb{P}_2}[s_{1t^*}^{w}|\mathcal{F}_t]}.$$

Further, we can obtain

$$
\begin{aligned}
E^{\mathbb{P}_1}[s_{1t^*}^w|\mathcal{F}_t] &= E^{\mathbb{Q}}[\frac{e^{-\int_t^T r_s ds+(m-w)y_{1T}+wy_{1t^*}}}{\Phi(t,T,t^*,y,v,r,-i(m-w),0,0)}|\mathcal{F}_t] = \frac{\Phi(t,T,t^*,y,v,r,-i(m-w),0,-iw)}{\Phi(t,T,t^*,y,v,r,-i(m-w),0,0)},\\
E^{\mathbb{P}_2}[s_{1t^*}^w|\mathcal{F}_t] &= E^{\mathbb{Q}}[\frac{e^{-\int_t^T r_s ds+(m-w)y_{1T}+y_{2T}+wy_{1t^*}}}{\Phi(t,T,t^*,y,v,r,-i(m-w),-i,0)}|\mathcal{F}_t] = \frac{\Phi(t,T,t^*,y,v,r,-i(m-w),-i,-iw)}{\Phi(t,T,t^*,y,v,r,-i(m-w),-i,0)}.
\end{aligned}
$$

The situation of P_3 and P_4 can be verified through similar reasoning as in Theorem 3.1.

Next, define the joint characteristic functions of $(y_{1T}, y_{2T}, y_{1t^*})$ under the new measure P_3 and P_4,

$$
\varphi_3(u_1,u_2,u_3) = E^{\mathbb{P}_3}[e^{iu_1y_{1T}+iu_2y_{2T}+iu_3y_{1t^*}}|\mathcal{F}_t],
$$

$$
\varphi_4(u_1,u_2,u_3) = E^{\mathbb{P}_4}[e^{iu_1y_{1T}+iu_2y_{2T}+iu_3y_{1t^*}}|\mathcal{F}_t],
$$

where (u_1,u_2,u_3) represents coefficient variations of $(y_{1T}, y_{2T}, y_{1t^*})$.
The new joint characteristic functions under the new probability measures P_3, P_4 are given by

$$
\begin{aligned}
\varphi_3(u_1,u_2,u_3) =&\ E^{\mathbb{P}_1}[\frac{e^{iu_1y_{1T}+iu_2y_{2T}+(w+iu_3)y_{1t^*}}}{E^{\mathbb{P}_1}[s_{1t^*}^w|\mathcal{F}_t]}|\mathcal{F}_t]\\
=&\ E^{\mathbb{Q}}[\frac{e^{-\int_t^T r_s ds+((m-w)+iu_1)y_{1T}+iu_2y_{2T}+(w+iu_3)y_{2T}}}{\Phi(t,T,t^*,y,v,r,-i(m-w),0,0)E^{\mathbb{P}_1}[S_{1t^*}^w|\mathcal{F}_t]}|\mathcal{F}_t]\\
=&\ \frac{\Phi(t,T,t^*,y,v,r,u_1-i(m-w),u_2,u_3-iw)}{\Phi(t,T,t^*,y,v,r,-i(m-w),0,-iw)},\\
\varphi_4(u_1,u_2,u_3) =&\ E^{\mathbb{P}_2}[\frac{e^{iu_1y_{1T}+iu_2y_{2T}+(w+iu_3)y_{1t^*}}}{E^{\mathbb{P}_2}[s_{1t^*}^w|\mathcal{F}_t]}|\mathcal{F}_t]\\
=&\ E^{\mathbb{Q}}[\frac{e^{-\int_t^T r_s ds+((m-w)+iu_1)y_{1T}+(1+iu_2)y_{2T}+(w+iu_3)y_{2T}}}{\Phi(t,T,t^*,y,v,r,-i(m-w),-i,0)E^{\mathbb{P}_1}[S_{1t^*}^w|\mathcal{F}_t]}|\mathcal{F}_t]\\
=&\ \frac{\Phi(t,T,t^*,y,v,r,u_1-i(m-w),u_2-i,u_3-iw)}{\Phi(t,T,t^*,y,v,r,-i(m-w),-i,-iw)}.
\end{aligned}
$$

Further, by applying the joint characteristic functions $\varphi_3(u_1,u_2,u_3)$, $\varphi_4(u_1,u_2,u_3)$, we obtain the final result

$$
\begin{aligned}
&V_2(t,T,m,w|s,v,r)\\
=&\ \Phi(t,T,t^*,y,v,r,-i(m-w),0,-iw)E^{\mathbb{P}_3}[1_{\{s_{2T}\geq D^*\}}|\mathcal{F}_t]\\
&+\tfrac{(1-\varpi)}{D}\Phi(t,T,t^*,y,v,r,-i(m-w),-i,-iw)E^{P_4}[1_{\{s_{2T}<D^*\}}|\mathcal{F}_t]\\
=&\ \Phi(t,T,t^*,y,v,r,-i(m-w),0,-iw)P_3\{y_{2T}\geq \ln D^*|\mathcal{F}_t\}\\
&+\tfrac{(1-\varpi)}{D}\Phi(t,T,t^*,y,v,r,-i(m-w),-i,-iw)P_4\{y_{2T}<\ln D^*|\mathcal{F}_t\}\\
=&\ \Phi(t,T,t^*,y,v,r,-i(m-w),0,-iw)F(\ln D^*,\varphi_3(0,u,0))\\
&+\tfrac{(1-\varpi)}{D}\Phi(t,T,t^*,y,v,r,-i(m-w),-i,-iw)F(-\ln D^*,\varphi_4(0,-u,0)).
\end{aligned}
$$

In a similar line to $\triangle_2(t,T,m,w|s,v,r)$, we can obtain $(y_1 = \ln(s_1))$:

$$
\triangle_2(t,T,m,w|s,v,r) = \frac{\partial V_2(t,T,m,w|s,v,r)}{\partial s_1} = \frac{\partial V_2(t,T,m,w|s,v,r)}{\partial y_1}\cdot\frac{1}{s_1} = \frac{\partial V_2(t,T,m,w|s,v,r)}{\partial y_1}\cdot e^{-y_1}.
$$

According to the expression of $\Phi(t,T,t^*,y,v,r,u)$ in Theorem 2.5, we can obtain

$$
\frac{\partial\Phi(t,T,t^*,y,v,r,-i(m-w),0,-iw)}{\partial y_1} = m\Phi(t,T,t^*,y,v,r,-i(m-w),0,-iw),
$$

$$
\frac{\partial\Phi(t,T,t^*,y,v,r,-i(m-w),-i,-iw)}{\partial y_1} = m\Phi(t,T,t^*,y,v,r,-i(m-w),-i,-iw).
$$

From the expression of $\varphi_3(u_1, u_2, u_3)$ and $\varphi_4(u_1, u_2, u_3)$, it can be further known that $\varphi_3(0, u, 0)$ and $\varphi_4(0, -u, 0)$ do not contain variable y_1. Therefore, the following facts hold true:

$$\frac{\partial F(\ln D^*, \varphi_3(0, u, 0)}{\partial y_1} = \frac{\partial F(-\ln D^*, \varphi_4(0, -u, 0))}{\partial y_1} = 0.$$

Continue to differentiate and substitute the above conclusion; then, we can obtain the final result.

$$\begin{aligned}
& \triangle_2(t, T, m, w|s, v, r) \\
= \;& m\Phi(t, T, t^*, y, v, r, -i(m-w), 0, -iw) \cdot e^{-y_1} \cdot F(\ln D^*, \varphi_3(0, u, 0)) \\
& + \tfrac{(1-\varpi)}{D} m\Phi(t, T, t^*, y, v, r, -i(m-w), -i, -iw) \cdot e^{-y_1} \cdot F(-\ln D^*, \varphi_4(0, -u, 0)).
\end{aligned}$$

□

4. Application of the Laplace–Fourier transform

In this section, we will construct the Laplace–Fourier combination algorithm based on the theoretical foundation established in Section 2, and the pricing formula derived in Section 3. It is worth noting that, on the one hand, in order to ensure the existence of the Fourier part, the attenuation coefficient needs to be set; on the other hand, in order to ensure the efficient asymptotic expansion of the Laplace part, it is necessary to determine the expansion starting point. The specific process of algorithm is as follows: Steps 1–3 are mainly the construction of an inverse Fourier transform, and are the further improvement and perfection of Carr's research results [31]. Steps 4 and 5 are mainly the construction of an inverse Laplace transform.

Step 1. Rely on measure transformation and decomposition techniques: The computation of V_1, V_2 is simplified as follows. Let $d^* = \ln D^*$,

$$\begin{aligned}
& V_1(t, T, m, w|s, v, r) \\
= \;& \varphi(t, T, y, v, r, -i(m-w), 0, 0, 0, 0) E^{\mathbb{P}_1}[1_{\{y_{2T} \geq d^*\}}|\mathcal{F}_t] \\
& + \tfrac{(1-\varpi)}{D} \varphi(t, T, y, v, r, -i(m-w), -i, 0, 0, 0) E^{\mathbb{P}_2}[1_{\{y_{2T} < d^*\}}|\mathcal{F}_t], \\
= \;& \varphi(t, T, y, v, r, -i(m-w), 0, 0, 0, 0) \textstyle\int_{d^*}^{+\infty} q_1(y) dy \\
& + \tfrac{(1-\varpi)}{D} \varphi(t, T, y, v, r, -i(m-w), -i, 0, 0, 0) \textstyle\int_{-\infty}^{d^*} q_2(y) dy \\
= \;& \varphi(t, T, y, v, r, -i(m-w), 0, 0, 0, 0) \Pi_1(d^*) \\
& + \tfrac{(1-\varpi)}{D} \varphi(t, T, y, v, r, -i(m-w), -i, 0, 0, 0) \Pi_2(d^*), \\
& V_2(t, T, m, w|s, v, r) \\
= \;& \Phi(t, T, t^*, y, v, r, -i(m-w), 0, -iw) E^{\mathbb{P}_3}[1_{\{y_{2T} \geq d^*\}}|\mathcal{F}_t] \\
& + \tfrac{(1-\varpi)}{D} \Phi(t, T, t^*, y, v, r, -i(m-w), -i, -iw) E^{P_4}[1_{\{y_{2T} < d^*\}}|\mathcal{F}_t], \\
= \;& \Phi(t, T, t^*, y, v, r, -i(m-w), 0, -iw) \textstyle\int_{d^*}^{+\infty} q_3(y) dy \\
& + \tfrac{(1-\varpi)}{D} \Phi(t, T, t^*, y, v, r, -i(m-w), -i, -iw) \textstyle\int_{-\infty}^{d^*} q_4(y) dy \\
= \;& \Phi(t, T, t^*, y, v, r, -i(m-w), 0, -iw) \Pi_3(d^*) \\
& + \tfrac{(1-\varpi)}{D} \Phi(t, T, t^*, y, v, r, -i(m-w), -i, -iw) \Pi_4(d^*),
\end{aligned}$$

where $q_i(y), i = 1, 2, 3, 4$ represent the corresponding probability density functions. Subsequently, the asymptotic computation of the probability terms $\Pi_k(d^*), k = 1, 2, 3, 4$ is mainly considered.

Step 2. Under the condition that the attenuation coefficient is set, Fourier transform is implemented, and its corresponding inverse Fourier transform is given. The group of formulas is the Fourier transform formula of the key term after the decay operation,

$$\begin{aligned}
\pi_1^*(u) &= \int_{-\infty}^{+\infty} e^{(iu+\epsilon_1)d^*}\Pi_1(d^*)dd^* = +\tfrac{\varphi_1(0,u-i\epsilon_1)}{iu+\epsilon_1}, \epsilon_1 > 0,\\
\pi_2^*(u) &= \int_{-\infty}^{+\infty} e^{(iu+\epsilon_2)d^*}\Pi_2(d^*)dd^* = -\tfrac{\varphi_2(0,u-i\epsilon_2)}{iu+\epsilon_2}, \epsilon_2 < 0,\\
\pi_3^*(u) &= \int_{-\infty}^{+\infty} e^{(iu+\epsilon_3)d^*}\Pi_3(d^*)dd^* = +\tfrac{\varphi_3(0,u-i\epsilon_3,0)}{iu+\epsilon_3}, \epsilon_3 > 0,\\
\pi_4^*(u) &= \int_{-\infty}^{+\infty} e^{(iu+\epsilon_4)d^*}\Pi_4(d^*)dd^* = -\tfrac{\varphi_4(0,u-i\epsilon_4,0)}{iu+\epsilon_4}, \epsilon_4 < 0.
\end{aligned}$$

Next, taking $\Pi_1(d^*)$ as an example, in order to ensure the existence of the corresponding Fourier transform, the derivation of the interval range of the damping coefficient ϵ_1 will be presented. The determination of other damping coefficients can be obtained in a similar manner.

Based on the expression of $\Pi_1(d^*)$, performing a Fourier transform on the variables d^* yields

$$\pi_1^*(u) = \int_{-\infty}^{+\infty} e^{iud^*}\cdot e^{\epsilon_1 d^*}\cdot \Pi_1(d^*)dd^* = \int_{-\infty}^{+\infty} e^{(iu+\epsilon_1)d^*}\Pi_1(d^*)dd^*.$$

Substituting into the expression of $\Pi_1(d^*)$ and the commutability of expectations and integration, it can be further obtained that

$$\begin{aligned}
\pi_1^*(u) &= \int_{-\infty}^{+\infty} e^{(iu+\epsilon_1)d^*}\cdot E^{\mathbb{P}_1}[1_{\{y_{2T}\geq d^*\}}|\mathcal{F}_t]dd^*\\
&= E^{\mathbb{P}_1}[\int_{-\infty}^{+\infty} e^{(iu+\epsilon_1)d^*}\cdot 1_{\{y_{2T}\geq d^*\}}dd^*|\mathcal{F}_t].
\end{aligned}$$

According to the variable separation method, we can obtain

$$\int_{-\infty}^{+\infty} e^{(iu+\epsilon_1)d^*}\cdot 1_{\{y_{2T}\geq d^*\}}dd^* = \int_{-\infty}^{y_{2T}} e^{(iu+\epsilon_1)d^*}dd^*.$$

In order to ensure the integrability of $\int_{-\infty}^{y_{2T}} e^{(iu+\epsilon_1)d^*}dd^*$, the condition $\epsilon_1 > 0$ is required. Under this condition, the result of the integration is as follows:

$$\int_{-\infty}^{y_{2T}} e^{(iu+\epsilon_1)d^*}dd^* = \frac{e^{(iu+\epsilon_1)y_{2T}}}{iu+\epsilon_1}.$$

Substitute the calculated terms $\int_{-\infty}^{y_{2T}} e^{(iu+\epsilon_1)d^*}dd^*$ into the formula $\pi_1^*(u)$ and then, based on the definition of the characteristic function, the final expression can be obtained:

$$\pi_1^*(u) = E^{\mathbb{P}_1}[\frac{e^{(iu+\epsilon_1)y_{2T}}}{iu+\epsilon_1}|\mathcal{F}_t] = +\frac{\varphi_1(0,u-i\epsilon_1)}{iu+\epsilon_1}, \epsilon_1 > 0.$$

In the meantime, the following formula is the corresponding inverse Fourier transform:

$$\Pi_k(d^*) = \tfrac{e^{-\epsilon_k d^*}}{2\pi}\int_{-\infty}^{+\infty} e^{-iud^*}\pi_k^*(u)du, k = 1,2,3,4.$$

Step 3. Discretize the inverse Fourier transform formula. The approximate formula for specific discretization is as follows:

$$\Pi_k(d^*) \approx \tfrac{e^{-\epsilon_k d^*}}{2\pi}\int_{-\frac{M_1}{2}}^{\frac{M_1}{2}} e^{-iud^*}\pi_k^*(u)du \approx \tfrac{e^{-\epsilon_k d^*}}{2\pi}\tfrac{M_1}{N_1}\sum_{j=0}^{N_1}\omega_j e^{-iu_j d^*}\pi_k^*(u_j), k = 1,2,3,4,$$

where $u_j = -\frac{M_1}{2} + \frac{jM_1}{N_1} = \frac{M_1(2j-N_1)}{2N_1}$, M_1 represents the approximate span, and N_1 represents the discrete fineness. If $j = 1, \cdots, N_1 - 1$, then $\omega_j = 1$; if $j = 0, N_1$, then $\omega_j = \frac{1}{2}$.

The following equivalent expression can be obtained by further simplification and collation:

$$\Pi_k(d^*) \approx \frac{M_1}{2\pi \cdot N_1} e^{(i\frac{M_1}{2}-\epsilon_k)d^*} \sum_{j=0}^{N_1} \omega_j e^{-i\frac{jM_1 d^*}{N_1}} \pi_k^*(\frac{M_1(2j-N_1)}{2N_1}), k = 1, 2, 3, 4.$$

Step 4. The inverse Laplace transforms are implemented. The above steps obtain the asymptotic solution of V_1, V_2. In combination with the beta function, the approximate semi-analytical solutions of the Laplace transform of vulnerable powered options are produced.

$$\begin{aligned}
C_1(t,T,m,K|s,v,r) &= \frac{1}{2\pi i}\int_{c-i\infty}^{c+i\infty} e^{wk}B(-w,m+1)\cdot V_1(t,T,m,w|s,v,r)dw, c<0,\\
P_1(t,T,m,K|s,v,r) &= \frac{1}{2\pi i}\int_{c-i\infty}^{c+i\infty} e^{wk}B(m-w,m+1)\cdot V_1(t,T,m,w|s,v,r)dw, c<m;\\
C_2(t,T,m,K|s,v,r) &= \frac{1}{2\pi i}\int_{c-i\infty}^{c+i\infty} e^{wk}B(-w,m+1)\cdot V_2(t,T,m,w|s,v,r)dw, c<0,\\
P_2(t,T,m,K|s,v,r) &= \frac{1}{2\pi i}\int_{c-i\infty}^{c+i\infty} e^{wk}B(m-w,m+1)\cdot V_2(t,T,m,w|s,v,r)dw, c<m,
\end{aligned}$$

where c is the starting point of the inverse Laplace transform expansion. For the choice of starting point, we can refer to Theorems 2.1 and 2.2.

Step 5. The discrete Laplace transforms are constructed. The following steps obtain the asymptotic solution of $C_i, P_i (i = 1, 2)$. The following formula gives the result of the discrete Laplace transform:

$$\begin{aligned}
C_1(t,T,m,K|s,v,r) &\approx \frac{1}{2\pi i}\int_{c-i\frac{M_2}{2}}^{c+i\frac{M_2}{2}} e^{wk}B(-w,m+1)\cdot V_1(t,T,m,w|s,v,r)dw\\
&\approx \frac{M_2}{2\pi\cdot N_2}\sum_{n=0}^{N_2} e^{w_n\cdot k}B(-w_n,m+1)\cdot V_1(t,T,m,w_n|s,v,r),\\
P_1(t,T,m,K|s,v,r) &\approx \frac{1}{2\pi i}\int_{c-i\frac{M_2}{2}}^{c+i\frac{M_2}{2}} e^{wk}B(m-w,m+1)\cdot V_1(t,T,m,w|s,v,r)dw\\
&\approx \frac{M_2}{2\pi\cdot N_2}\sum_{n=0}^{N_2} e^{w_n\cdot k}B(m-w_n,m+1)\cdot V_1(t,T,m,w_n|s,v,r);\\
C_2(t,T,m,K|s,v,r) &\approx \frac{1}{2\pi i}\int_{c-i\frac{M_2}{2}}^{c+i\frac{M_2}{2}} e^{wk}B(-w,m+1)\cdot V_2(t,T,m,w|s,v,r)dw\\
&\approx \frac{M_2}{2\pi\cdot N_2}\sum_{n=0}^{N_2} e^{w_n\cdot k}B(-w_n,m+1)\cdot V_2(t,T,m,w_n|s,v,r),\\
P_2(t,T,m,K|s,v,r) &\approx \frac{1}{2\pi i}\int_{c-i\frac{M_2}{2}}^{c+i\frac{M_2}{2}} e^{wk}B(m-w,m+1)\cdot V_2(t,T,m,w|s,v,r)dw\\
&\approx \frac{M_2}{2\pi\cdot N_2}\sum_{n=0}^{N_2} e^{w_n\cdot k}B(m-w_n,m+1)\cdot V_2(t,T,m,w_n|s,v,r),
\end{aligned}$$

where $w_n = c - i\frac{M_2}{2} + i\frac{nM_2}{N_2} = c + i\frac{M_2(2n-N_2)}{2N_2}$, M_2 represents the approximate span, and N_2 represents the discrete fineness.

5. Numerical example

In this section, we will obtain the calculation results of the asymptotic pricing formula of vulnerable powered options derived in Section 4, and further discuss the influence mechanism of stochastic interest rates and stochastic volatility on the pricing performance and risk hedging through the results. In order to ensure the accuracy of the calculation, MATLAB 2021a is used for program design. The detailed values of the key coefficients used by the model are shown in the Table 1 below. According to the evolution law of financial markets, let $f(v_1, v_2) = e^{\alpha_1 v_1 + \alpha_2 v_2}$, $g(v_1, v_2) = e^{\beta_1 v_1 + \beta_2 v_2}$, $\alpha_1 = \frac{1}{3}$, $\alpha_2 = \frac{2}{3}$, $\beta_1 = \frac{2}{3}$, $\beta_2 = \frac{1}{3}$. The total differential linearization method used in this paper is applicable to all multivariate differentiable functions. Therefore, for the volatility functions f and g, any differentiable functions of the variables v_1 and v_2 can be selected. The reason for choosing the above exponential-type volatility functions lies in two aspects. First, it results from the methodology adopted in [32]. Second, extensive empirical research has shown that asset return volatility exhibits characteristics such as clustering, volatility smile, and heavy tails, which can be effectively captured by exponential functions. Without loss of generality, the following analysis takes call options as experimental objects to test the pricing ability of the composite algorithm, where $M_1 = M_2 = 200$, $N_1 = N_2 = 2000$. It is necessary to clearly state here that, considering the differences in the structures and types of the two types of options (C_1, P_1) and (C_2, P_2), the selection of the strike price K also has significant differences in magnitude. Therefore, when calculating C_1 and P_1, the strike price $K = K_1$ is chosen; when calculating C_2 and P_2, the strike price $K = K_2$ is chosen. The basic parameter settings for the numerical experiments in this paper are mainly derived from the experimental data of previous researchers. Specifically, the parameter settings for the volatility factor are based on the structural data of [16], the initial data of the assets and the parameters of the jump structure are designed according to the calibration data of [2], and all the time data are in years.

Table 1. Parameter values for numerical experiments.

parameter	s_1	s_2	r	v_1	v_2	σ_r	σ_1	σ_2	θ_r	θ_1	θ_2	k_r	k_1	k_2	m
value	10	10	0.01	0.05	0.01	0.1	0.1	0.1	0.03	0.5	0.1	0.5	1	10	3
parameter	ρ_{12}	ρ_{1v_1}	ρ_{2v_1}	ρ_{1v_2}	ρ_{2v_2}	T	t^*	t	λ_0	λ_1	λ_2	α	β	γ	ϖ
value	0.2	0.5	0.5	-0.5	-0.5	1	0.5	0	2	3	3	0.5	0.5	0.5	0.5
parameter	μ_1	μ_2	$\sigma_{J_{01}}$	$\sigma_{J_{02}}$	$\rho_{J_1 J_2}$	p_1	ξ_1	η_1	p_2	ξ_2	η_2	K_1	K_2	D^*	D
value	0	0	0.1	0.1	0.5	0.6	12	14	0.64	18	21	10	1	7	7

In order to present the calibration method of the two-factor general stochastic volatility model proposed in this paper in detail, the implementation idea of the Monte Carlo algorithm is shown. It should be noted that in the subsequent numerical experiments, all the Monte Carlo algorithms are based on the original nonlinear model, rather than the approximate model. First, under actual market data, the stochastic differential equation system satisfied by the underlying asset, the two volatility factors, and the interest rate within the validity period of the option is discretized. The specific results are as follows:

$$\begin{aligned}
s_{1t_i} &= s_{1t_{i-1}} + s_{1t_{i-1}}[(r_t - \lambda_0 m_{01} - \lambda_1 m_{11})\Delta t + f(v_{1t_{i-1}}, v_{2t_{i-1}})\sqrt{\Delta t}\cdot\epsilon_1 \\
&\quad + (e^{J_{01}} - 1)(N_{0t_i} - N_{0t_{i-1}}) + (e^{J_{11}} - 1)(N_{1t_i} - N_{1t_{i-1}})], \\
s_{2t_i} &= s_{2t_{i-1}} + s_{2t_{i-1}}[(r_t - \lambda_0 m_{02} - \lambda_1 m_{12})\Delta t + g(v_{1t_{i-1}}, v_{2t_{i-1}})\sqrt{\Delta t}\cdot\epsilon_2 \\
&\quad + (e^{J_{02}} - 1)(N_{0t_i} - N_{0t_{i-1}}) + (e^{J_{12}} - 1)(N_{2t_i} - N_{2t_{i-1}})], \\
v_{1t_i} &= v_{1t_{i-1}} + k_1(\theta_1 - v_{1t_{i-1}})\Delta t + \sigma_1 v_{1t_{i-1}}^{\alpha}\sqrt{\Delta t}\cdot\epsilon_3, \\
v_{2t_i} &= v_{2t_{i-1}} + k_2(\theta_2 - v_{2t_{i-1}})\Delta t + \sigma_2 v_{2t_{i-1}}^{\beta}\sqrt{\Delta t}\cdot\epsilon_4, \\
r_{t_i} &= r_{t_{i-1}} + k_r(\theta_r - r_{t_{i-1}})\Delta t + \sigma_r r_{t_{i-1}}^{\gamma}\sqrt{\Delta t}\cdot\epsilon_5,
\end{aligned}$$

where $N_{jt_i} - N_{jt_{i-1}} \sim P(\lambda_j \cdot \Delta t)$, $j = 0, 1, 2$ are independent of each other, and $\epsilon_i \sim N(0, 1), i = 1, 2, 3, 4, 5$. The dependence structure of random variables $(\epsilon_1, \epsilon_2, \epsilon_3, \epsilon_4, \epsilon_5)$ is equivalent to the dependence structure of Brownian motion $(W_{1t}, W_{2t}, W_{1t}^{(v)}, W_{2t}^{(v)}, W_{rt})$. The program used here is MATLAB 2021a. Below is the implementation process for the jump structure in $[t_{i-1}, t_i]$. First, use the command *poissrnd*() to generate three independent Poisson random variables $(N_{0t_i} - N_{0t_{i-1}}, N_{1t_i} - N_{1t_{i-1}}, N_{2t_i} - N_{2t_{i-1}})$. Second, based on the value of $N_{0t_i} - N_{0t_{i-1}}$, determine the generation of the common jump vector (J_{01}, J_{02}). If $N_{0t_i} - N_{0t_{i-1}} = 0$, this indicates no common jumps; if $N_{0t_i} - N_{0t_{i-1}} = 1$, generate a two-dimensional normal random variable (J_{01}, J_{02}) using the command *mvnrnd*(); if $N_{0t_i} - N_{0t_{i-1}} = n$, generate n independent two-dimensional normal random variables (J_{01}, J_{02}) and sum them up to determine the common jump magnitudes for the two assets (s_{1t_i}, s_{2t_i}). Finally, based on the value of $N_{1t_i} - N_{1t_{i-1}}$ and $N_{2t_i} - N_{2t_{i-1}}$, determine the generation of the individual jump vectors (J_{11}, J_{12}). Take $N_{1t_i} - N_{1t_{i-1}}$ as an example to illustrate the generation process J_{11}. Regarding $N_{2t_i} - N_{2t_{i-1}}$ and J_{12}, similar results can be obtained. If $N_{1t_i} - N_{1t_{i-1}} = 0$, it indicates that there is no individual jump; if $N_{1t_i} - N_{1t_{i-1}} = 1$, apply command *rand*() to generate a uniformly distributed random variable X, and at the same time, determine the range of X. If $X > p_1$, then apply a command *exprnd*() to generate an exponential distribution random variable Y, which is $J_{11} = Y$. If $X \leq p_1$, then apply a command *exprnd*() to generate an exponential distribution random variable Y, which is $J_{11} = -Y$. If $N_{1t_i} - N_{1t_{i-1}} = n$, repeat the independent generation of n times according to the case of $N_{1t_i} - N_{1t_{i-1}} = 1$ and accumulate them to finally determine the individual jump amplitude of asset s_{1t_i}. The random seed settings are as follows: The generator type is of the Generator class, the generator bit number is G64 bit, and the random seed value is 12345. In the Monte Carlo simulation algorithm, we employ the variance reduction technique for the dual variables. Additionally, let the number of random walks be 100, that is, $\Delta t = \frac{T-t}{100}$.

Next, taking the volatility factor as an example, the basic strategies for parameter estimation and market calibration are presented. The parameters for other factors can be given in a similar manner. Considering that the price of assets consists of two components: diffusion and jump, and these two parts are independent of each other, a separate estimation approach is adopted. This paper selects the stock price data of two listed companies, such as Gree Electric Appliances and Haier Electric Appliances, to calibrate the volatility. The specific sample for calibration is the hourly closing price data of 251 trading days throughout 2025. At the same time, the closing price data is converted into return data, and the Lee–Myland method [33] is used to detect the jump points of the return data and the average return data of the two. With the help of the function $findchangepts()$ in MATLAB, the structural breakpoints in the return sequence, including individual jump points and common jump points, are identified. At the same time, the entire price data is decomposed into diffusion sample data and jump sample data.

Next, based on the previous 10 data points, the historical volatility data of the two assets is calculated. Combining the functional form of volatility, the least squares method is applied to obtain the time series data of the potential volatility factors. Finally, the maximum likelihood estimation method is used, and the MATLAB function *mle*() is utilized to obtain the parameter results of the two volatility factors. It should be noted that the market calibration of the risk associated with dependent jump structures can be carried out using similar methods and approaches. Therefore, no further elaboration will be provided on this matter.

Table 2 presents the convergence data of the Monte Carlo algorithm under different simulation path numbers. First, in general, as the simulation number increases, the prices of all vulnerable powered options tend to stabilize. Therefore, to ensure the accuracy of the Monte Carlo reference algorithm, in all the subsequent comparative experiments, we have adopted the highest path number of 2000. Second, from the perspective of the power parameter, as the power exponent increases, the leverage of the corresponding option also increases, the price stability decreases, and the simulation number requirement also increases. Finally, from the efficiency perspective, the Monte Carlo algorithm often requires more computing time under high-precision requirements. However, the Laplace–Fourier transform algorithm provides the asymptotic semi-analytical expression of the option, so the cost of computing time is minimal. This is also the main advantage of this paper in conducting the corresponding theoretical demonstration.

Table 2. The convergence properties of the MC method.

m	0.5	1	1.5	2	2.5	3	3.5	4	4.5
C_1(N=50)	0.1074	0.2343	0.5952	1.7039	5.4920	19.1509	73.1126	300.8247	1331.3029
C_1(N=100)	0.1072	0.2324	0.5921	1.7077	5.4564	19.0540	72.6111	300.8036	1334.3094
C_1(N=200)	0.1069	0.2323	0.5926	1.7070	5.4612	19.1136	72.7587	300.8552	1337.5869
C_1(N=500)	0.1070	0.2325	0.5932	1.7092	5.4628	19.1192	72.8732	300.8321	1335.8920
C_1(N=1000)	0.1070	0.2325	0.5930	1.7072	5.4570	19.1036	72.8397	300.5920	1335.4382
C_1(N=2000)	0.1070	0.2325	0.5930	1.7078	5.4594	19.1011	72.8451	300.5456	1335.0159
C_2(N=50)	0.1006	0.2086	0.5131	1.4224	4.5616	16.0414	63.5044	275.3606	1311.4371
C_2(N=100)	0.1010	0.2103	0.5120	1.4377	4.5771	16.0993	63.6517	276.4224	1310.3776
C_2(N=200)	0.1014	0.2102	0.5126	1.4312	4.5835	16.1843	63.8732	277.4421	1314.4076
C_2(N=500)	0.1013	0.2098	0.5127	1.4319	4.5786	16.1485	63.8362	277.2672	1310.9242
C_2(N=1000)	0.1013	0.2099	0.5125	1.4326	4.5758	16.1536	63.8355	277.4476	1312.1335
C_2(N=2000)	0.1013	0.2099	0.5126	1.4332	4.5752	16.1563	63.8053	277.3825	1311.8722

In order to investigate the pricing accuracy of proposed algorithm, Monte Carlo simulation is used as the reference algorithm in this part to compare and analyze the pricing gap and absolute error rate. Starting from two vulnerable powered options, Table 3 presents the pricing results and hedging results of two algorithms, respectively. The experimental results indicate that the Laplace–Fourier algorithm has outstanding pricing ability and more accurate pricing levels in general. Specifically, on the one hand, in terms of absolute error rate, the pricing error of the Laplace–Fourier algorithm is almost always below 1%, and rarely exceeds this range. On the other hand, in terms of the absolute error, the error will gradually expand as the power increases, reflecting the destabilizing effect of the leverage of the power operation on pricing behavior; that is, as the power increases, the option price shows explosive growth. Therefore, further caution is needed regarding the pricing and investment of high-powered options.

Next, in order to further verify the reliability and effectiveness of the Laplace–Fourier combined algorithm proposed in this paper under high-precision requirements for pricing, we set the reference algorithm (the Monte Carlo simulation algorithm) with 10^5 as the base sample path. If the standard deviation of the Monte Carlo simulation price at 10^5 is lower than $\frac{1}{1000}$ of the mean value, then the final algorithm mean, standard deviation, and CPU running time will be output, which will be used as the comparison algorithm for this paper's algorithm. Meanwhile, the Laplace–Fourier algorithm adopts the method of gradually expanding the truncation interval. Following the idea of expanding the interval length by one time each time until the relative error between the price calculated by this paper's algorithm and the price of the Monte Carlo algorithm is less than $\frac{1}{1000}$, the price of the combined algorithm and the CPU running time will be output.

Table 3. Numerical comparison under Monte Carlo (MC) and Laplace–Fourier (LF).

m	0.5	1	1.5	2	2.5	3	3.5	4	4.5
C_1(LF)	0.1068	0.2327	0.5927	1.7067	5.4517	19.0902	72.7152	299.7527	1333.0192
C_1(MC)	0.1070	0.2325	0.5930	1.7078	5.4594	19.1011	72.8451	300.5456	1335.0159
APE(%)	0.19%	0.09%	0.05%	0.07%	0.14%	0.06%	0.18%	0.26%	0.15%
Δ_1(LF)	0.0322	0.0847	0.2492	0.8068	2.8447	10.8471	44.5312	196.2621	927.0770
Δ_1(MC)	0.0325	0.0841	0.2480	0.8101	2.8334	10.8472	44.4370	195.0638	936.0749
APE(%)	0.94%	0.64%	0.47%	0.40%	0.40%	0.00%	0.21%	0.61%	0.96%
C_2(LF)	0.1014	0.2083	0.5092	1.4336	4.5589	16.1838	63.6354	275.7582	1312.8518
C_2(MC)	0.1013	0.2099	0.5126	1.4332	4.5752	16.1563	63.8053	277.3825	1311.8722
APE(%)	0.10%	0.75%	0.66%	0.02%	0.36%	0.17%	0.27%	0.59%	0.07%
Δ_2(LF)	0.0051	0.0208	0.0764	0.2867	1.1397	4.8551	22.2724	110.3033	590.7833
Δ_2(MC)	0.0051	0.0211	0.0769	0.2865	1.1428	4.8459	22.3419	111.3530	591.3425
APE(%)	0.20%	1.22%	0.66%	0.06%	0.27%	0.19%	0.31%	0.94%	0.09%

Table 4 presents a comparison of the pricing results obtained by the Monte Carlo simulation algorithm and the Laplace–Fourier combined algorithm under a high-precision requirement. First, from the perspective of the pricing result data, the standard deviations of the reference algorithm's results are all relatively small, thereby ensuring the accuracy of the reference results. At the same time, under the condition of continuously expanding the truncation interval, the combined algorithm can also achieve the same high-precision level. Second, from the perspective of CPU time consumption for pricing, at the same high-precision level, the combined algorithm proposed in this paper requires less computing time, which is also the main advantage of the Laplace–Fourier combined transformation. Finally, because the pricing method proposed in this paper is a linear approximation method, it has a better pricing effect, which requires the volatility function to have a good behavior and the volatility factor to change smoothly. Once these conditions are destroyed, the effect of the algorithm will be unimaginable, which is the limitation of this method.

Table 4. Numerical comparison of MC and LF under a high-precision requirement.

m	0.5	1	1.5	2	2.5	3	3.5	4
C_1(MC)	0.1084	0.2333	0.5928	1.7066	5.4552	19.0839	72.7738	300.2452
std(MC)	0.0001	0.0002	0.0004	0.0010	0.0046	0.0102	0.0565	0.0627
TCs(MC)	448.0587	434.6192	400.7196	498.2769	386.3392	457.3885	393.9508	337.5872
C_1(LF)	0.1076	0.2327	0.5943	1.7078	5.4548	19.0828	72.7723	300.2454
TCs(LF)	59.6339	71.0297	72.4759	148.9547	69.4882	112.9409	146.0629	77.9129
C_2(MC)	0.1021	0.2102	0.5126	1.4324	4.5707	16.1407	63.7434	277.1069
std(MC)	0.0000	0.0002	0.0005	0.0012	0.0022	0.0009	0.0596	0.1335
TCs(MC)	370.5720	472.1198	302.2957	500.2390	351.3675	510.4325	475.4740	321.1500
C_2(LF)	0.1025	0.2107	0.5126	1.4330	4.5721	16.1419	63.7428	277.1053
TCs(MC)	110.3123	123.5837	57.1329	50.1921	79.3637	111.3319	108.5038	121.8598

Table 5 presents the pricing data of the classical Black-Scholes (B-S) model and the Laplace–Fourier combined transformation algorithm under the condition of $m = 1$. The last column shows the theoretical analytical solution of the call option of the B-S model. As the initial price s_2 of the counterparty's asset gradually increases, the future risk of the counterparty's default gradually decreases. Therefore, when $s_2 \to \infty$ holds true, the price of the vulnerable option tends to be the price of the European option. From the pricing results of the Laplace–Fourier combined transformation algorithm and the analytical results of the call option, this algorithm can better approximate the exact price of the option under the degenerate model. To a certain extent, this indicates the scientificity and effectiveness of the pricing of the Laplace–Fourier algorithm.

Table 5. Numerical comparison of MC and LF under the B-S model.

s_2	10	50	100	500	1000	B-S
$C_1(K = 15)$	0.0100	0.0100	0.0098	0.0093	0.0097	0.0090
$C_1(K = 10)$	1.0925	1.2220	1.2764	1.2819	1.2828	1.2822
$C_1(K = 5)$	4.1588	4.8513	5.2536	5.3201	5.3202	5.3251
$C_2(K = 2)$	0.0540	0.0696	0.1044	0.1262	0.1285	0.1271
$C_2(K = 1)$	0.5684	0.7480	0.9807	1.0790	1.0838	1.0841
$C_2(K = 0.5)$	3.0689	3.8443	4.5697	4.7990	4.8062	4.8110

Table 6 presents the pricing data of the classical Heston model and the Laplace–Fourier combined transformation algorithm under the condition of $m = 1$. The last column shows the integral solution of the call option in the Heston model. As the risk boundary D^* gradually decreases, the future risk of counterparty default gradually decreases. Therefore, when $D^* \to 0$ holds, the price of vulnerable options tends to be the price of European options. From the pricing results of the Laplace–Fourier combined transformation algorithm and the analytical results of the call option, this algorithm can better approximate the exact price of the option under the degenerate Heston model. To a certain extent, this indicates the rationality and feasibility of the Laplace–Fourier combined algorithm in pricing the traditional Heston model.

Table 6. Numerical comparison of MC and LF under the Heston model.

D^*	200	100	50	20	10	0	Heston
$C_1(s_1 = 5)$	0.1168	0.1785	0.197	0.2005	0.2009	0.2012	0.2012
$C_1(s_1 = 10)$	1.0437	1.7224	2.0023	2.0617	2.0693	2.0741	2.0747
$C_1(s_1 = 15)$	3.9692	6.8179	8.5136	8.9773	9.045	9.0896	9.0964
$C_2(s_1 = 5)$	0.4166	0.6685	0.7611	0.7791	0.7813	0.7827	0.7828
$C_2(s_1 = 10)$	2.0181	3.4175	4.0735	4.2226	4.2421	4.2548	4.2564
$C_2(s_1 = 15)$	5.424	9.321	11.8485	12.6263	12.7493	12.835	12.8483

5.1. Numerical analysis for vulnerable powered European options

In this subsection, we continue to apply Laplace–Fourier composite algorithm and further discuss the pricing behavior and hedging characteristics of vulnerable powered European call options. The following numerical analysis mainly focuses on two volatility factors (long-term and short-term), risk-free interest rate, and strike price.

First, Tables 7 and 8 respectively show the evolution path of option prices under different key parameters α, β of two volatility factors v_{1t}, v_{2t}. Bbcause of the volatility factor v_{1t} playing a leading role in the determination of asset volatility and the exponential hypothesis of $f(v_{1t}, v_{2t})$ and $g(v_{1t}, v_{2t})$, the variance of the volatility factor v_{1t} continues to enlarge, and the growth rate of option prices keeps rising as α eventually tends to 0 from 1. Because the volatility factor v_{2t} plays a fine-tuning role in the determination of asset volatility, the growth rate of option prices is relatively stable as β eventually tends to 0 from 1. This point can be more vividly verified by Figure 1. In addition, the leverage of power is also the cause of the rapid change of pricing results.

Table 7. Vulnerable powered European call option prices under different α and m.

(α, m)	0.5	1	1.5	2	2.5	3	3.5	4	4.5
0	0.1181	0.3018	0.9191	3.2224	12.7549	56.3131	275.1916	1481.3058	8758.0963
0.1	0.1116	0.2638	0.7354	2.3379	8.3123	32.6548	140.6341	660.5833	3373.4676
0.2	0.1086	0.2446	0.6465	1.9385	6.4693	23.7427	95.0760	413.2881	1943.8950
0.3	0.1076	0.2381	0.6168	1.8097	5.8996	21.1149	82.3220	347.8440	1587.8009
0.4	0.1071	0.2348	0.6018	1.7455	5.6197	19.8458	76.2792	317.4764	1426.2346
0.5	0.1068	0.2327	0.5927	1.7067	5.4517	19.0902	72.7152	299.7527	1333.0192
0.6	0.1067	0.2314	0.5866	1.6805	5.3387	18.5843	70.3408	288.0154	1271.7050
0.7	0.1065	0.2304	0.5821	1.6616	5.2570	18.2190	68.6313	279.5958	1227.9125
0.8	0.1064	0.2297	0.5788	1.6472	5.1948	17.9412	67.3331	273.2164	1194.8284
0.9	0.1064	0.2291	0.5761	1.6358	5.1457	17.7216	66.3081	268.1876	1168.8035
1	0.1063	0.2287	0.5740	1.6266	5.1057	17.5430	65.4749	264.1041	1147.7036

Table 8. Vulnerable powered European call option prices under different β and m.

(β, m)	0.5	1	1.5	2	2.5	3	3.5	4	4.5
0	0.1069	0.2327	0.5920	1.7025	5.4301	18.9810	72.1547	296.7835	1316.6123
0.1	0.1069	0.2327	0.5921	1.7032	5.4336	18.9989	72.2462	297.2656	1319.2640
0.2	0.1069	0.2327	0.5923	1.7044	5.4397	19.0296	72.4031	298.0949	1323.8358
0.3	0.1069	0.2327	0.5925	1.7053	5.4446	19.0543	72.5302	298.7687	1327.5610
0.4	0.1069	0.2327	0.5926	1.7061	5.4485	19.0743	72.6327	299.3136	1330.5810
0.5	0.1068	0.2327	0.5927	1.7067	5.4517	19.0902	72.7152	299.7527	1333.0192
0.6	0.1068	0.2327	0.5928	1.7072	5.4542	19.1031	72.7813	300.1056	1334.9814
0.7	0.1068	0.2328	0.5928	1.7075	5.4562	19.1133	72.8343	300.3885	1336.5563
0.8	0.1068	0.2328	0.5929	1.7078	5.4578	19.1215	72.8766	300.6148	1337.8177
0.9	0.1068	0.2328	0.5929	1.7081	5.4591	19.1280	72.9104	300.7957	1338.8263
1	0.1068	0.2328	0.5930	1.7083	5.4601	19.1332	72.9374	300.9400	1339.6317

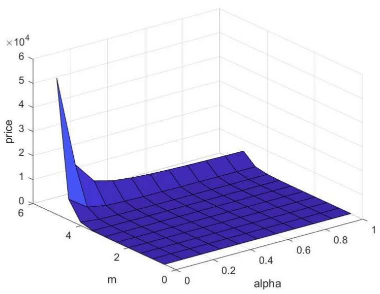

(a) m and α

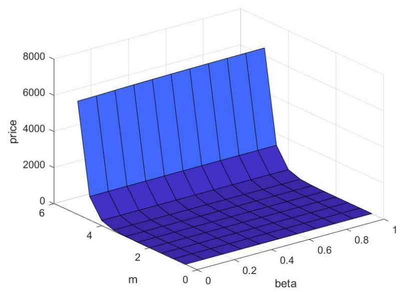

(b) m and β

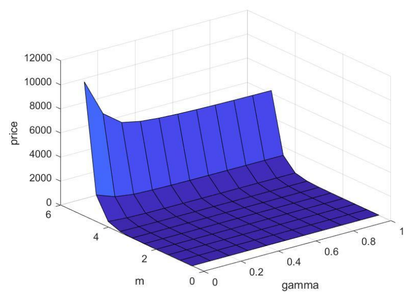

(c) m and γ

Figure 1. The surface of vulnerable powered European call option prices.

Second, Table 9 presents the mechanism by which the key parameter of the risk-free rate affects the option price. Combined with Figure 1, it can be concluded that the risk-free interest rate is another key factor in option pricing. The reason is that in the risk-neutral pricing principle, the expected return rate of all assets is the risk-free interest rate r_t, so the interest rate has a fundamental impact on option pricing. Compared with the two volatility factors, v_{1t} is the most sensitive to the impact of option pricing, followed by r_t and v_{2t}.

Table 9. Vulnerable powered European call option prices under different γ and m.

(γ, m)	0.5	1	1.5	2	2.5	3	3.5	4	4.5
0	0.1217	0.2795	0.7484	2.2614	7.5724	27.7778	110.8008	478.2523	2227.0449
0.1	0.1136	0.2531	0.6584	1.9348	6.3037	22.5028	87.3482	366.8437	1661.7216
0.2	0.1094	0.2402	0.6164	1.7875	5.7490	20.2640	77.6795	322.2117	1441.6236
0.3	0.1080	0.2360	0.6030	1.7417	5.5795	19.5920	74.8253	309.2487	1378.7060
0.4	0.1073	0.2340	0.5965	1.7196	5.4987	19.2742	73.4868	303.2152	1349.6332
0.5	0.1068	0.2327	0.5927	1.7067	5.4517	19.0902	72.7152	299.7527	1333.0192
0.6	0.1066	0.2319	0.5902	1.6982	5.4209	18.9704	72.2139	297.5097	1322.2846
0.7	0.1064	0.2314	0.5884	1.6922	5.3993	18.8860	71.8619	295.9370	1314.7709
0.8	0.1062	0.2309	0.5871	1.6877	5.3831	18.8233	71.6007	294.7718	1309.2096
0.9	0.1061	0.2306	0.5860	1.6843	5.3707	18.7749	71.3991	293.8726	1304.9216
1	0.1060	0.2303	0.5852	1.6815	5.3607	18.7363	71.2385	293.1572	1301.5111

Tables 10 and 11 present the pricing results and hedging shares of options at different strike prices, respectively. On the whole, the option prices and the hedge shares tend to be the same, which can be seen more clearly from Figure 2. Specifically, as the strike price K increases, option prices decrease and so do hedging shares, but the proportion of changes in the hedging share is larger; especially, the power m is higher, showing nonconsistency. In other words, the lower the power m, the lower the proportion of hedging variation; the higher the power m, the higher the proportion of hedging changes.

Table 10. Vulnerable powered European call option prices under different K and m.

(K, m)	0.5	1	1.5	2	2.5	3	3.5	4	4.5
5	0.2907	0.7312	2.0407	6.2139	20.4432	72.2326	273.0636	1101.8961	4740.8400
6	0.2505	0.6030	1.6346	4.8814	15.8617	55.6539	209.8263	847.4553	3660.3476
7	0.2097	0.4870	1.2895	3.7938	12.2194	42.6992	160.9360	651.8363	2830.9095
8	0.1710	0.3861	1.0044	2.9234	9.3641	32.6740	123.3728	501.9597	2194.9590
9	0.1364	0.3015	0.7745	2.2384	7.1514	24.9735	94.6382	387.3490	1707.3358
10	0.1068	0.2327	0.5927	1.7067	5.4517	19.0902	72.7152	299.7527	1333.0192
11	0.0826	0.1781	0.4513	1.2980	4.1543	14.6105	56.0078	232.7595	1045.0935
12	0.0632	0.1354	0.3425	0.9863	3.1681	11.2053	43.2728	181.4392	823.0049
13	0.0480	0.1026	0.2596	0.7497	2.4201	8.6176	33.5539	142.0298	651.1252
14	0.0363	0.0776	0.1967	0.5706	1.8533	6.6496	26.1211	111.6743	517.5996
15	0.0274	0.0586	0.1493	0.4353	1.4236	5.1501	20.4209	88.2100	413.4434

Table 11. Vulnerable powered European call option deltas under different K and m.

(K,m)	0.5	1	1.5	2	2.5	3	3.5	4	4.5
5	0.0340	0.1396	0.5241	1.9740	7.6617	30.9906	131.3479	585.2236	2747.7712
6	0.0371	0.1340	0.4706	1.6999	6.4173	25.4826	106.7487	472.5514	2213.6874
7	0.0386	0.1249	0.4136	1.4405	5.3115	20.7766	86.2651	380.2923	1780.8578
8	0.0381	0.1128	0.3559	1.2024	4.3498	16.8183	69.4000	305.3406	1431.8735
9	0.0358	0.0990	0.3003	0.9905	3.5304	13.5359	55.6503	244.8444	1151.5857
10	0.0322	0.0847	0.2492	0.8068	2.8447	10.8471	44.5312	196.2621	927.0770
11	0.0280	0.0709	0.2039	0.6514	2.2796	8.6667	35.5967	157.3900	747.5305
12	0.0238	0.0584	0.1651	0.5223	1.8196	6.9123	28.4514	126.3610	604.0256
13	0.0197	0.0475	0.1326	0.4168	1.4488	5.5092	22.7555	101.6235	489.2965
14	0.0161	0.0382	0.1058	0.3314	1.1519	4.3916	18.2238	81.9073	397.4824
15	0.0130	0.0305	0.0841	0.2630	0.9156	3.5038	14.6214	66.1848	323.8907

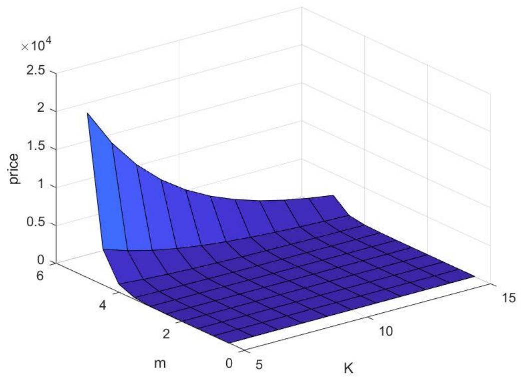

(a) Prices

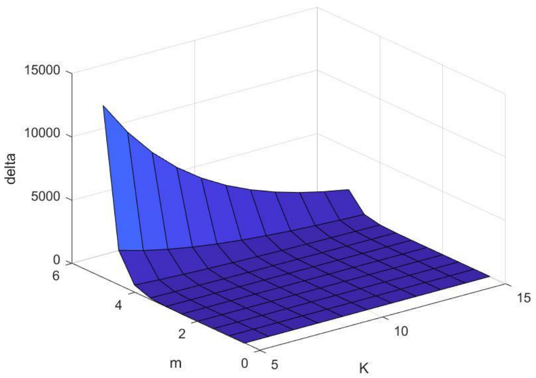

(b) Deltas

Figure 2. The surface of vulnerable powered European call option prices and Δ_1

Table 12 presents the pricing results of vulnerable powered options under different volatility levels. The volatilities of both assets are jointly driven by two market volatility factors, where the macro volatility factor mainly characterizes the systematic modulation of the overall economic market or financial market on the volatility of assets, and the micro volatility factor mainly characterizes the intrinsic characteristics or price movement patterns of the underlying assets on the volatility of assets. On one hand, from a general perspective, as the value of the two market volatility factors continue to increase, the price of the option also rises. The reason for this is that the volatility provides a space for the price of the underlying assets to change, providing the possibility for the option to achieve excess returns. On the other hand, by comparing the influence degrees of the two, it can be clearly seen that the macro market factor has a more profound impact on the option price. This also indicates that when conducting related investment work on powered options, more attention should be paid to the occurrence and patterns of macro market volatility phenomena.

Table 12. Vulnerable powered European call option prices under different v_1 and v_2.

(v_1, v_2)	0.025	0.05	0.075	0.1	0.125	0.15	0.175	0.2
0.0025	14.6345	15.5930	17.3978	20.1486	24.0865	29.6067	37.3109	48.0974
0.005	14.9376	15.9159	17.7581	20.5659	24.5853	30.2199	38.0836	49.0936
0.0075	15.4843	16.4985	18.4081	21.3187	25.4852	31.3260	39.4776	50.8905
0.01	16.2586	17.3234	19.3285	22.3846	26.7595	32.8923	41.4514	53.4350
0.0125	17.2634	18.3940	20.5231	23.7681	28.4133	34.9252	44.0133	56.7375
0.015	18.5146	19.7271	22.0105	25.4907	30.4725	37.4564	47.2031	60.8495
0.0175	20.0381	21.3504	23.8217	27.5882	32.9800	40.5386	51.0873	65.8567
0.02	21.8700	23.3023	25.9995	30.1104	35.9951	44.2446	55.7578	71.8774

5.2. Numerical analysis for vulnerable powered forward start options

In this subsection, we will continue to apply the Laplace–Fourier composite algorithm to analyze the pricing situation of another vulnerable powered option (vulnerable powered forward start options). This part of the experiment mainly discusses the impact of two volatility factors (long-term and short-term), risk-free interest rate, forward moment, and strike price on option pricing and hedging risk.

First, Tables 13–15 respectively show the evolution surfaces of corresponding option prices when the key parameters α, β, γ of two volatility factors and risk-free interest rate are valued regularly. Compared with the evolution of the first type of option, the evolution surface of the second type of option is similar. The long-run volatility factor and the risk-free rate still play a strong key role, and the short-run volatility factor still bears a fine-tuning role. However, it is worth noting that the strength of the volatility factor v_{1t} lags behind that of the risk-free interest rate. At the same time, the price of the second type is much lower than that of the first, which can be further verified by Figure 3. This is due to the fact that the payoff function of the forward option itself has a certain risk-hedging property, which weakens the leverage of the power m to some extent.

Table 13. Vulnerable powered forward start call option prices under different α and m.

(α, m)	0.5	1	1.5	2	2.5	3	3.5	4	4.5
0	0.1122	0.2607	0.7343	2.4249	9.2078	39.7263	193.2696	1055.1500	6446.0771
0.1	0.1121	0.2605	0.7325	2.4099	9.0970	38.9302	187.4065	1009.7696	6071.3972
0.2	0.1074	0.2376	0.6309	1.9439	6.8174	26.8844	118.2721	577.4425	3118.6658
0.3	0.1044	0.2229	0.5689	1.6778	5.6102	21.0133	87.4711	402.5755	2041.936
0.4	0.1026	0.2141	0.5326	1.5281	4.9593	17.9903	72.3799	321.3211	1569.0160
0.5	0.1014	0.2083	0.5092	1.4336	4.5589	16.1838	63.6354	275.7582	1312.8518
0.6	0.1006	0.2042	0.4929	1.3687	4.2891	14.9898	57.9768	246.9252	1154.5045
0.7	0.0999	0.2011	0.4809	1.3214	4.0952	14.1441	54.0297	227.1351	1047.6478
0.8	0.0994	0.1988	0.4717	1.2855	3.9492	13.5144	51.1242	212.7455	970.9432
0.9	0.0991	0.1969	0.4644	1.2573	3.8354	13.0274	48.8980	201.8253	913.3154
1	0.0988	0.1954	0.4584	1.2345	3.7441	12.6397	47.1384	193.2608	868.4844

Table 14. Vulnerable powered forward start call option prices under different β and m.

(β, m)	0.5	1	1.5	2	2.5	3	3.5	4	4.5
0	0.1017	0.2092	0.5122	1.4441	4.5985	16.3417	64.3127	278.8771	1328.2791
0.1	0.1016	0.2090	0.5115	1.4414	4.5879	16.2978	64.1153	277.9211	1323.2766
0.2	0.1015	0.2085	0.5100	1.4362	4.5678	16.2156	63.7543	276.2124	1314.5560
0.3	0.1014	0.2084	0.5096	1.4346	4.5622	16.1941	63.6673	275.8381	1312.8567
0.4	0.1014	0.2083	0.5094	1.4339	4.5600	16.1866	63.6415	275.7542	1312.6435
0.5	0.1014	0.2083	0.5092	1.4336	4.5589	16.1838	63.6354	275.7582	1312.8518
0.6	0.1014	0.2083	0.5092	1.4334	4.5584	16.1827	63.6360	275.7889	1313.1643
0.7	0.1014	0.2082	0.5091	1.4332	4.5581	16.1824	63.6388	275.8241	1313.4708
0.8	0.1014	0.2082	0.5091	1.4331	4.5579	16.1822	63.6417	275.8557	1313.7338
0.9	0.1014	0.2082	0.5090	1.4331	4.5577	16.1822	63.6441	275.8810	1313.9438
1	0.1014	0.2082	0.5090	1.4330	4.5576	16.1821	63.6457	275.8997	1314.1029

Table 15. Vulnerable powered forward start call option prices under different γ and m.

(γ, m)	0.5	1	1.5	2	2.5	3	3.5	4	4.5
0	0.0984	0.2195	0.5981	1.9328	7.2989	32.0167	163.1573	971.0997	6824.8052
0.1	0.1010	0.2173	0.5623	1.6942	5.8367	22.7502	99.7295	490.2687	2701.7069
0.2	0.1024	0.2124	0.5245	1.4918	4.7936	17.1983	68.3625	299.5468	1442.3649
0.3	0.1020	0.2103	0.5163	1.4590	4.6574	16.5956	65.4991	284.8921	1361.3677
0.4	0.1016	0.2091	0.5120	1.4433	4.5961	16.3376	64.3250	279.1087	1330.5061
0.5	0.1014	0.2083	0.5092	1.4336	4.5589	16.1838	63.6354	275.7582	1312.8518
0.6	0.1012	0.2077	0.5073	1.4269	4.5335	16.0793	63.1705	273.5138	1301.0921
0.7	0.1011	0.2073	0.5059	1.4219	4.5149	16.0033	62.8332	271.8902	1292.6107
0.8	0.1010	0.2069	0.5048	1.4182	4.5007	15.9453	62.5764	270.6567	1286.1781
0.9	0.1009	0.2067	0.5040	1.4152	4.4895	15.8995	62.3741	269.6861	1281.1229
1	0.1008	0.2065	0.5033	1.4127	4.4804	15.8625	62.2105	268.9020	1277.0422

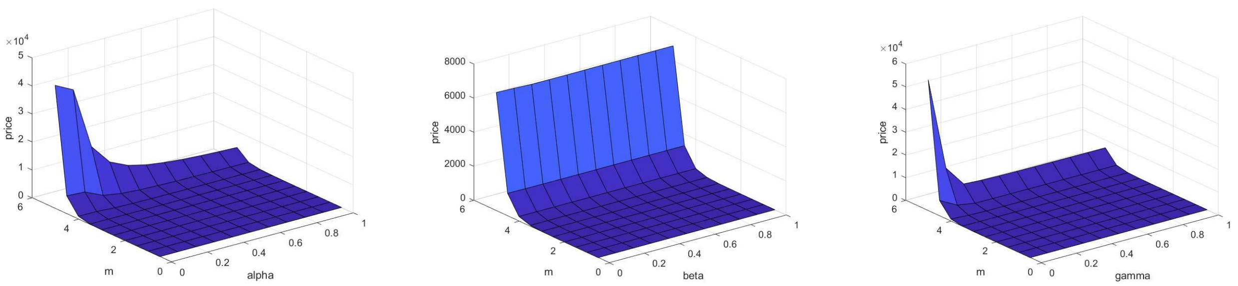

(a) m and α (b) m and β (c) m and γ

Figure 3. The surface of vulnerable powered forward start call option prices.

Second, Tables 16 and 17 show option pricing and risk hedging at different forward moments respectively. Obviously, in Figure 4, as the forward moment t_1 changes from the initial time t to the maturity time T, the price of the second type changes from the value of European option to 0, and the corresponding hedging share also decreases to 0. Similarly, the power m plays an important role in leverage. Therefore, the pricing and investment of such high-powered options also need in-depth investigation, selection, and hedging to avoid the subsequent high risks.

Table 16. Vulnerable powered forward start call option prices under different t_1 and m.

(t_1, m)	0.5	1	1.5	2	2.5	3	3.5	4	4.5
0	0.1149	0.2795	0.8033	2.6341	9.6620	39.1532	173.8589	841.3894	4422.3255
0.1	0.1135	0.2716	0.7681	2.4812	8.9737	35.8892	157.4303	753.3402	3918.8361
0.2	0.1113	0.2595	0.7159	2.2595	7.9986	31.3683	135.1792	636.6911	3266.2114
0.3	0.1086	0.2447	0.6539	2.0028	6.8952	26.3590	110.9892	512.0194	2579.1189
0.4	0.1053	0.2277	0.5846	1.7245	5.7320	21.2100	86.6776	389.1718	1913.4416
0.5	0.1014	0.2083	0.5092	1.4336	4.5589	16.1838	63.6354	275.7582	1312.8518
0.6	0.0966	0.1863	0.4283	1.1365	3.4154	11.4909	42.9576	177.5923	809.5959
0.7	0.0906	0.1610	0.3416	0.8384	2.3372	7.3170	25.5440	99.0078	425.0292
0.8	0.0825	0.1307	0.2478	0.5444	1.3627	3.8457	12.1584	42.9050	168.7268
0.9	0.0700	0.0914	0.1431	0.2606	0.5436	1.2880	3.4503	10.4346	35.6550

Table 17. Powered forward start call option deltas under different t_1 and m.

(t_1, m)	0.5	1	1.5	2	2.5	3	3.5	4	4.5
0	0.0057	0.0280	0.1205	0.5268	2.4155	11.7460	60.8506	336.5558	1990.0465
0.1	0.0057	0.0272	0.1152	0.4962	2.2434	10.7668	55.1006	301.3361	1763.4763
0.2	0.0056	0.0259	0.1074	0.4519	1.9996	9.4105	47.3127	254.6764	1469.7951
0.3	0.0054	0.0245	0.0981	0.4006	1.7238	7.9077	38.8462	204.8078	1160.6035
0.4	0.0053	0.0228	0.0877	0.3449	1.4330	6.3630	30.3372	155.6687	861.0487
0.5	0.0051	0.0208	0.0764	0.2867	1.1397	4.8551	22.2724	110.3033	590.7833
0.6	0.0048	0.0186	0.0642	0.2273	0.8539	3.4473	15.0351	71.0369	364.3181
0.7	0.0045	0.0161	0.0512	0.1677	0.5843	2.1951	8.9404	39.6031	191.2632
0.8	0.0041	0.0131	0.0372	0.1089	0.3407	1.1537	4.2554	17.1620	75.9271
0.9	0.0035	0.0091	0.0215	0.0521	0.1359	0.3864	1.2076	4.1738	16.0448

Tables 18 and 19 present the pricing results and hedging shares of the second type options at different strike prices, respectively. Compared with the first type, it can be found that the change trend and transformation shape of two type options are basically similar in Figure 5. However, as K is valued regularly downward, the proportion of the evolution of option price and hedge share on the second type is larger, and the gap between the two increases. This is due to the multiplicity of forward option payoff functions and the dual effect of powered options, which make the space of pricing and the width of hedging extended to a certain extent.

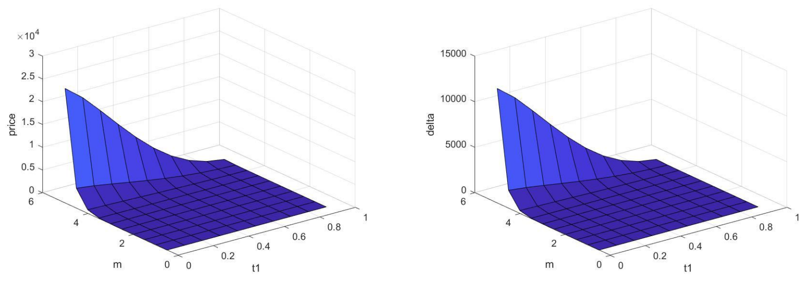

(a) Prices (b) Deltas

Figure 4. The surface of vulnerable powered forward start call option prices and delta under m and t_1

Table 18. Vulnerable powered forward start call option price under different K and m.

(K, m)	0.5	1	1.5	2	2.5	3	3.5	4	4.5
0.5	0.2975	0.7367	2.0484	6.3020	21.2675	78.3077	313.5052	1361.8851	6412.9052
0.6	0.2562	0.6012	1.6098	4.8199	15.9515	57.9379	229.8898	993.6384	4670.9659
0.7	0.2130	0.4774	1.2384	3.6261	11.8162	42.4802	167.5417	722.3254	3397.1751
0.8	0.1711	0.3696	0.9348	2.6896	8.6637	30.9290	121.5779	524.0362	2470.5989
0.9	0.1334	0.2800	0.6944	1.9723	6.3024	22.4071	87.9998	379.9854	1798.9112
1	0.1014	0.2083	0.5092	1.4336	4.5589	16.1838	63.6354	275.7582	1312.8518
1.1	0.0756	0.1528	0.3699	1.0355	3.2861	11.6731	46.0377	200.5124	961.2105
1.2	0.0554	0.1109	0.2668	0.7450	2.3645	8.4206	33.3613	146.2237	706.5503
1.3	0.0402	0.0799	0.1916	0.5348	1.7010	6.0825	24.2388	107.0272	521.7321
1.4	0.0289	0.0573	0.1373	0.3838	1.2250	4.4040	17.6712	78.6750	387.1967
1.5	0.0207	0.0409	0.0983	0.2756	0.8841	3.1988	12.9355	58.1103	288.8980

Table 19. Vulnerable powered forward start call option delta under different K and m.

(K, m)	0.5	1	1.5	2	2.5	3	3.5	4	4.5
0.5	0.0149	0.0737	0.3073	1.2604	5.3169	23.4923	109.7268	544.7540	2885.8073
0.6	0.0128	0.0601	0.2415	0.9640	3.9879	17.3814	80.4614	397.4554	2101.9346
0.7	0.0106	0.0477	0.1858	0.7252	2.9540	12.7441	58.6396	288.9302	1528.7288
0.8	0.0086	0.0370	0.1402	0.5379	2.1659	9.2787	42.5523	209.6145	1111.7695
0.9	0.0067	0.0280	0.1042	0.3945	1.5756	6.7221	30.7999	151.9942	809.5100
1	0.0051	0.0208	0.0764	0.2867	1.1397	4.8551	22.2724	110.3033	590.7833
1.1	0.0038	0.0153	0.0555	0.2071	0.8215	3.5019	16.1132	80.2050	432.5447
1.2	0.0028	0.0111	0.0400	0.1490	0.5911	2.5262	11.6765	58.4895	317.9476
1.3	0.0020	0.0080	0.0287	0.1070	0.4253	1.8248	8.4836	42.8109	234.7795
1.4	0.0014	0.0057	0.0206	0.0768	0.3063	1.3212	6.1849	31.4700	174.23854
1.5	0.0010	0.0041	0.0147	0.0551	0.2210	0.9597	4.5274	23.2441	130.0041

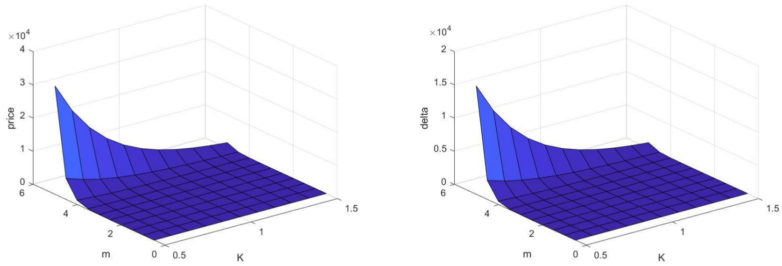

(a) Prices (b) Deltas

Figure 5. The surface of powered forward start call option prices and delta under m and K.

6. Conclusions

In this paper, by using the Laplace–Fourier combination algorithm, the pricing issue of two types of vulnerable options under the general stochastic volatility model is discussed. On one hand, the pricing and risk hedging of options are studied in the case of complex price mechanisms. On the other hand, the Laplace–Fourier combination algorithm is proposed, making the pricing of these two types of vulnerable options more operable and obtaining the asymptotic solutions of options. Finally, the experimental results show that the proposed method can effectively solve the pricing problem of vulnerable power options in general stable financial market environments (non-high volatility or sudden-type volatility). This paper applies the total differential linearization method to solve the asymptotic pricing problem of two types of vulnerable powered options by transforming nonlinear partial differential equations into linear ones through Laplace–Fourier compound transforms. However, the total differential linearization method is essentially a local approximation technique, with clear applicability boundaries and limitations. First, its core application scenario involves small deviation analysis around a mean-reverting level or stable point, requiring two conditions to be met. The first condition is that the nonlinear function being linearized must be continuously differentiable, without discontinuities or abrupt jumps; the second condition is that the variation range of the approximated variable must be very small, operating within a narrow deviation from a given mean. Second, under these two conditions, this method can be extended to price various financial derivatives and conduct risk analysis in more complex financial market environments. Finally, the main limitation of this method lies in its accuracy being restricted by the magnitude of deviations. Approximation precision is sufficient only when the increment of the approximated variable is very small; as the increment increases, the error caused by neglecting higher-order terms becomes significantly larger, making it unsuitable for large deviation analyses. Moreover, it cannot be applied to discontinuous or highly nonlinear differential equation systems, for instance, systems involving discontinuities, saturation, or other nonsmooth nonlinear characteristics, where direct Taylor expansion fails to achieve effective linearization.

Author contributions

Libin Wang: Conceptualization, methodology, software; Ruonan Zhang: Validation, formal analysis, visualization.

Use of Generative-AI tools declaration

The authors state that they did not use any AI tools in the creation of this paper.

Acknowledgments

This work is funded by the Hebei Key Laboratory of Financial Technology Application (Grant No. 2024008). The authors would like to thank the referee who gave many valuable suggestions.

Conflict of interest

The authors declare that there is no conflict of interest with any institution in this paper.

References

1. P. Klein, Pricing Black-Scholes options with correlated credit risk, *J. Bank. Financ.*, **20** (1996), 1211–1229. http://doi.org/10.1016/0378-4266(95)00052-6
2. Q. Zhou, J. J. Yang, W. X. Wu, Pricing vulnerable options with correlated credit risk under jump-diffusion processes when corpoate liabilities are random, *Acta Math. Appl. Sin. Engl. Ser.*, **35** (2019), 305–318. https://doi.org/10.1007/s10255-019-0821-y
3. X. Wang, Valuing vulnerable options with two underlying assets, *Appl. Econ. Lett.*, **27** (2020), 1699–1706. https://doi.org/10.1080/13504851.2020.1713980
4. R. G. Tompkins, Power options: Hedging nonlinear risks, *J. Risk*, **2** (2000), 29–45. https://doi.org/10.21314/jor.2000.022
5. H. K. Xu, The valuation of powered options, *J. Nonlinear Convex A.*, **16** (2015), 1461–1471.
6. R. C. Heynen, H. M. Kat, Pricing and hedging power options, *Financ. Eng. Jap. Mark*, **3** (1996), 253–261. http://doi.org/10.1007/BF02425804
7. F. Black, M. S. Scholes, The pricing of options and corporate liablities, *J. Polit. Econ.*, **81** (1973), 637–654. http://doi.org/10.1086/260062
8. L. B. G. Andersen, V. V. Piterbarg, Moment explosions in stochastic volatility models, *Finance Stoch.*, **11** (2007), 29–50. http://doi.org/10.1007/s00780-006-0011-7
9. A. Esser, General valuation principles for arbitrary payoffs and applications to power options under stochastic volatility, *Financ. Mark. Portfoli.*, **17** (2003), 351–372. http://doi.org/10.1007/s11408-003-0305-0
10. J. Kim, B. Kim, K. S. Moon, I. S. Wee, Valuation of power options under Heston's stochastic volatility model, *J. Econ. Dyn. Control.*, **36** (2012), 1796–1813. http://doi.org/10.1016/j.jedc.2012.05.005
11. S. L. Heston, A closed-form solutions for options with stochastic volatility with applications to bond and currency options, *Rev. Financ. Stud.*, **6** (1993), 327–343. http://doi.org/10.1093/rfs/6.2.327

12. S. N. I. Ibrahim, J. G. O'Hara, N. Constantinou, Pricing power options under the Heston framework, *New Trends Math. Sci.*, **1** (2013), 1–9.

13. J. Kim, Pricing of power options under the regime-switching model, *J. Appl. Math. Inform.*, **32** (2014), 665–673. http://doi.org/10.14317/jami.2014.665

14. J. Kim, B. Kim, J. Kim, S. Lee, Computation of powered option prices under a general model for underlying asset dynamics, *J. Comput. Appl. Math.*, **406** (2022), 113999. http://doi.org/10.1016/j.cam.2021.113999

15. E. Dastranj, H. S. Fard, A. Abdolbaghi, S. R. Hejazi, Power option pricing under the unstable conditions (Evidence of power option pricing under fractional Heston model in the Iran gold market), *Physica. A.*, **537** (2020), 122690. http://doi.org/10.1016/j.physa.2019.122690

16. Y. Xie, G. Deng, Vulnerable European option pricing in a Markov regime-switching Heston model with stochastic interest rate, *Chaos Soliton. Fract.*, **156** (2022), 111896. http://doi.org/10.1016/j.chaos.2022.111896

17. S. Han, Y. Wei, Power options pricing under Markov Regime-switching two-factor stochastic volatility jump-diffusion model, *Chin. Quart. J. Math.*, **40** (2025), 59–73.

18. L. Wang, L. Liu, Pricing vulnerable reset options under stochastic volatility jump diffusion model using 3-D FFT, *Commun. Stat.-Theor. M.*, **54** (2025), 4791–4818. http://doi.org/10.1080/03610926.2024.2427233

19. P. Christoffersen, S. Heston, K. Jacobs, The shape and term structure of the index option s-mirk: Why multifactor stochastic volatility models work so well, *Manage. Sci.*, **55** (2009), 1914–1932. http://doi.org/10.1287/mnsc.1090.1065

20. Y. M. Lian, J. H. Chen, S. L. Liao, Cojump risks and their impacts on option pricing, *Q. Rev. Econ. Financ.*, **79** (2021), 399–410. http://doi.org/10.1016/j.qref.2020.07.009

21. T. Liu, F. Soleymani, Z. M. Ullah, Solving multi-dimensional European option pricing problems by integrals of the inverse quadratic radial basis function on non-uniform meshes, *Chaos Soluton. Fract.*, **185** (2024), 115156. http://doi.org/10.1016/j.chaos.2024.115156

22. T. Liu, T. Li, Z. U. Malik, On five-point equidistant stencils based on Gaussian function with application in numerical multi-dimensional option pricing, *Comput. Math. Appl.*, **176** (2024), 35–45. http://doi.org/10.1016/j.camwa.2024.09.003

23. T. Liu, B. Ding, F. Soleymani, Risk quantification using Rayleigh-Tail modeling framework: A theoretical study and numerical simulations, *Comput. Appl. Math.*, **45** (2026), 173. http://doi.org/10.1007/s40314-025-03477-4

24. Y. Liu, Y. Li, T. Liu, An RBF-FD method for pricing under the Bates model: Handling stochastic volatility and jump processes, *Eng. Anal. Bound. Elem.*, **183** (2026), 106622. http://doi.org/10.1016/j.enganabound.2025.106622

25. T. Liu, B. Ding, A radial basis function neural network approach for solving a diffusion partial differential equation efficiently, *Appl. Math. Comput.*, **509** (2026), 129651. http://doi.org/10.1016/j.amc.2025.129651

26. J. Hull, A. White, The pricing of options on assets with stochastic volatilities, *J. Financ.*, **42** (1987), 281–300. http://doi.org/10.1111/j.1540-6261.1987.tb02568.x

27. R. C. Merton, Option pricing when underlying stock returns are discontinuous, *J. Financ. Econ.*, **3** (1976), 125–144. http://doi.org/10.1016/0304-405X(76)90022-2

28. S. G. Kou, A jump-diffusion model for option pricing, *Manage. Sci.*, **48** (2002), 1086–1101.

29. J. Hull, A. White, Pricing interest-rate-derivative securities, *Rev. Financ. Stud.*, **3** (1990), 573–592. http://doi.org/10.1093/rfs/3.4.573

30. S. Huang, X. Guo, Valuation of European-style vulnerable options under the non-affine stochastic volatility and double exponential jump, *Chaos Soluton. Fract.*, **158** (2022), 112003. http://doi.org/10.1016/j.chaos.2022.112003

31. P. Carr, D. B. Madan, Option valuation using the fast Fourier transform, *J. Comput. Financ.*, **2** (1999), 61–73. http://doi.org/10.21314/JCF.1999.043

32. J. Jeon, G. Kim, J. Huh, An asymptotic expansion approach to the valuation of vulnerable options under a multiscale stochastic volatility model, *Chaos Soluton. Fract.*, **144** (2021), 110641. http://doi.org/10.1016/j.chaos.2020.110641

33. S. S. Lee, P. A. Myland, Jumps in financial makerts: A new nonparametric test and jump dynamics, *Rev. Financ. Stud.*, **21** (2008), 2535–2563. http://doi.org/10.1093/rfs/hhm056

34. L. Teng, M. Ehrhardt, M.G. Unther, On the Heston model with stochastic correlation, *Int. J. Theor. Appl. Fin.*, **19** (2016), 1650033. http://doi.org/10.1142/S0219024916500333

Appendix: The proof of Lemma 2.1.

Proof. According to Itô's lemma and making the variable substitution $y_{1t} = \ln s_{1t}$, y_{1t} satisfies

$$dy_{1t} = (r_t - \lambda_0 m_{01} - \lambda_1 m_{11} - \tfrac{1}{2} f^2(v_{1t}, v_{2t}))dt + f(v_{1t}, v_{2t})dW_{1t} + J_{01}dN_{0t} + J_{11}dN_{1t}.$$

From the discounted martingale property of the asset, the term $M(t, T, y_1, v, r, n)$ satisfies a partial differential equation given by ($\tau = T - t$):

$$\begin{aligned}
&-\tfrac{\partial M}{\partial \tau} + (r - \lambda_0 m_{01} - \lambda_1 m_{11} - \tfrac{1}{2} f^2(v_1, v_2))\tfrac{\partial M}{\partial y_1} + \tfrac{1}{2} f^2(v_1, v_2)\tfrac{\partial^2 M}{\partial y_1^2} + k_1(\theta_1 - v_1)\tfrac{\partial M}{\partial v_1}\\
&+k_2(\theta_2 - v_2)\tfrac{\partial M}{\partial v_2} + k_r(\theta_r - r)\tfrac{\partial M}{\partial r} + \tfrac{1}{2}\sigma_1^2 v_1^{2\alpha}\tfrac{\partial^2 M}{\partial v_1^2} + \tfrac{1}{2}\sigma_2^2 v_2^{2\beta}\tfrac{\partial^2 M}{\partial v_2^2} + \tfrac{1}{2}\sigma_r^2 r^{2\gamma}\tfrac{\partial^2 M}{\partial r^2}\\
&+\rho_{1v_1} f(v_1, v_2) v_1^{\alpha}\tfrac{\partial^2 M}{\partial y_1 \partial v_1} + \rho_{1v_2} f(v_1, v_2) v_2^{\beta}\tfrac{\partial^2 M}{\partial y_1 \partial v_2} - (r + \lambda_0 + \lambda_1)M(t, T, y_1, v, r, n)\\
&+\lambda_0 E^{\mathbb{Q}}[M(t, T, y_1 + J_{01}, v, r, n)] + \lambda_1 E^{\mathbb{Q}}[M(t, T, y_1 + J_{11}, v, r, n)] = 0
\end{aligned}$$

with the boundary condition $M(T, T, y_1, v, r, n) = e^{ny_1}$.

By the technique of total differentiation of multivariate functions, the following approximate linear PDE can be derived:

$$\begin{aligned}
&-\tfrac{\partial M}{\partial \tau} + [r - \lambda_0 m_{01} - \lambda_1 m_{11} - \tfrac{1}{2}L_0(f, f) - \tfrac{1}{2}L_1(f, f)v_1 - \tfrac{1}{2}L_2(f, f)v_2]\tfrac{\partial M}{\partial y_1}\\
&+\tfrac{1}{2}[L_0(f, f) + L_1(f, f)v_1 + L_2(f, f)v_2]\tfrac{\partial^2 M}{\partial y_1^2} + k_1(\theta_1 - v_1)\tfrac{\partial M}{\partial v_1} + k_2(\theta_2 - v_2)\tfrac{\partial M}{\partial v_2} + k_r(\theta_r - r)\tfrac{\partial M}{\partial r}\\
&+\tfrac{1}{2}\sigma_1^2[(1 - 2\alpha)\theta_1^{2\alpha} + 2\alpha\theta_1^{2\alpha-1}v_1]\tfrac{\partial^2 M}{\partial v_1^2} + \tfrac{1}{2}\sigma_{2v}^2[(1 - 2\beta)\theta_2^{2\alpha} + 2\beta\theta_2^{2\beta-1}v_2]\tfrac{\partial^2 M}{\partial v_2^2}\\
&+\tfrac{1}{2}\sigma_r^2[(1 - 2\gamma)\theta_r^{2\gamma} + 2\gamma\theta_r^{2\gamma-1}r]\tfrac{\partial^2 M}{\partial r^2} + \rho_{1v_1}[L_0(f, v_1^{\alpha}) + L_1(f, v_1^{\alpha})v_1 + L_2(f, v_1^{\alpha})v_2]\tfrac{\partial^2 M}{\partial y_1 \partial v_1}\\
&+\rho_{1v_2}[L_0(f, v_1^{\beta}) + L_1(f, v_2^{\beta})v_1 + L_2(f, v_2^{\beta})v_2]\tfrac{\partial^2 M}{\partial y_1 \partial v_2} - (r + \lambda_0 + \lambda_1)M(t, T, y_1, v, r, n)\\
&+\lambda_0 E^{\mathbb{Q}}[M(t, T, y_1 + J_{01}, v, r, n)] + \lambda_1 E^{\mathbb{Q}}[M(t, T, y_1 + J_{11}, v, r, n)] = 0
\end{aligned}$$

with the boundary condition $M(T,T,y,v,r,u) = e^{ny_1}$.

Assume that $M(t,T,y_1,v,r,n)$ is of the form

$$M(t,T,y_1,v,r,n) = e^{ny_1+\widetilde{A}(\tau,n)+\widetilde{C}_1(\tau,n)v_1+\widetilde{C}_2(\tau,n)v_2+\widetilde{D}(\tau,n)r}.$$

Then, we obtain

$$\begin{aligned} E^{\mathbb{Q}}[M(t,T,y_1+J_{11},v,r,n)] &= M(t,T,y_1,v,r,n)E^{\mathbb{Q}}[e^{nJ_{11}}], \\ E^{\mathbb{Q}}[M(t,T,y_1+J_{01},v,r,n)] &= M(t,T,y_1,v,r,n)E^{\mathbb{Q}}[e^{nJ_{01}}]. \end{aligned}$$

Further, $\widetilde{A}(\tau,n)$, $\widetilde{C}_1(\tau,n)$, $\widetilde{C}_2(\tau,n)$, and $\widetilde{D}(\tau,n)$ become solutions of the Riccati differential equations

$\frac{\partial\widetilde{A}}{\partial\tau} = \lambda_0(E^{\mathbb{Q}}[e^{nJ_{01}}] - nm_{01} - 1) + \lambda_1(E^{\mathbb{Q}}[e^{nJ_{11}}] - nm_{11} - 1) - \frac{1}{2}L_0(f,f)(n-n^2)$
$+ [k_1\theta_1 + \rho_{1v_1}(L_0(f,v_1^{\alpha}) + L_2(f,v_1^{\alpha})\theta_2)n]\widetilde{C}_1 + [k_2\theta_2 + \rho_{1v_2}(L_0(f,v_2^{\beta}) + L_1(f,v_2^{\beta})\theta_1)n]\widetilde{C}_2$
$+ k_r\theta_r\widetilde{D} + \frac{1}{2}(1-2\alpha)\sigma_1^2\theta_1^{2\alpha}\widetilde{C}_1^2 + \frac{1}{2}(1-2\beta)\sigma_2^2\theta_2^{2\beta}\widetilde{C}_2^2 + \frac{1}{2}(1-2\gamma)\sigma_r^2\theta_r^{2\gamma}\widetilde{D}^2$,
$\frac{\partial\widetilde{C}_1}{\partial\tau} = \alpha\sigma_1^2\theta_1^{2\alpha-1}\widetilde{C}_1^2 - (k_1 - \rho_{1v_1}L_1(f,v_1^{\alpha})n)\widetilde{C}_1 - \frac{1}{2}L_1(f,f)(n-n^2)$,
$\frac{\partial\widetilde{C}_2}{\partial\tau} = \beta\sigma_2^2\theta_2^{2\beta-1}\widetilde{C}_2^2 - (k_2 - \rho_{1v_2}L_2(f,v_2^{\beta})n)\widetilde{C}_2 - \frac{1}{2}L_2(f,f)(n-n^2)$,
$\frac{\partial\widetilde{D}}{\partial\tau} = \gamma\sigma_r^2\theta_r^{2\gamma-1}\widetilde{D}^2 - k_rD + n - 1$,
with the boundary condition $\widetilde{A}(0,u) = 0, \widetilde{C}_1(0,u) = 0, \widetilde{C}_2(0,u) = 0, \widetilde{D}(0,u) = 0$. □

Appendix: The proof of Lemma 2.2.

Proof. The condition for the boundedness of $M(t,T,y_1,v,r,n)$ is verified below. To ensure its boundedness, it suffices to ensure the boundedness of the four terms $e^{\widetilde{C}_1(\tau,n)v_1}$, $e^{\widetilde{C}_2(\tau,n)v_2}$, $e^{\widetilde{D}(\tau,n)r}$, and $e^{\widetilde{A}(\tau,n)}$.

In the following, we first analyze the conditions for the boundedness of $e^{\widetilde{C}_1(\tau,n)v_1}$. Considering that the solution of $\widetilde{C}_1(\tau,n)$ with complex function form given by the above lemma is relatively simple but not suitable for analysis, the solution with real function form is given below:

$$\widetilde{C}_1(\tau,n) = \begin{cases} \frac{\widetilde{b}_1(n)+\sqrt{\widetilde{\delta}_1(n)}}{2\alpha\sigma_1^2\theta_1^{2\alpha-1}} \cdot \frac{1-e^{\sqrt{\widetilde{\delta}_1(n)}\tau}}{1-\widetilde{g}_1(n)e^{\sqrt{\widetilde{\delta}_1(n)}\tau}}, & \widetilde{\delta}_1(n) > 0; \\ \frac{\widetilde{b}_1^2(n)\tau}{2\alpha\sigma_1^2\theta_1^{2\alpha-1}(2+\widetilde{b}_1(n)\tau)}, & \widetilde{\delta}_1(n) = 0; \\ \frac{\sqrt{-\widetilde{\delta}_1(n)}}{2\alpha\sigma_1^2\theta_1^{2\alpha-1}}\tan(\frac{\sqrt{-\widetilde{\delta}_1(n)}}{2}\tau - \arctan\frac{\widetilde{b}_1(n)}{\sqrt{-\widetilde{\delta}_1(n)}}) + \frac{\widetilde{b}_1(n)}{2\alpha\sigma_1^2\theta_1^{2\alpha-1}}, & \widetilde{\delta}_1(n) < 0. \end{cases}$$

When $\widetilde{\delta}_1(n) > 0$, the equivalent condition for $e^{\widetilde{C}_1(\tau,n)v_1}$ to be bounded is $1 - \widetilde{g}_1(n)e^{\sqrt{\widetilde{\delta}_1(n)}\tau} \neq 0$.

Case 1. $|\widetilde{b}_1(n)| < \sqrt{\widetilde{\delta}_1(n)}$; then

$$\widetilde{g}_1(n) < 0 \Rightarrow 1 - \widetilde{g}_1(n)e^{\sqrt{\widetilde{\delta}_1(n)}\tau} > 0;$$

Case 2. $\widetilde{b}_1(n) > \sqrt{\widetilde{\delta}_1(n)}$; then

$$\widetilde{g}_1(n) > 1 \Rightarrow 1 - \widetilde{g}_1(n)e^{\sqrt{\widetilde{\delta}_1(n)}\tau} < 0;$$

Case 3. $-\widetilde{b}_1(n) > \sqrt{\widetilde{\delta}_1(n)}, -\ln \widetilde{g}_1(n) \geq \sqrt{\widetilde{\delta}_1(n)}\tau$; then

$$0 < \widetilde{g}_1(n) < 1 \Rightarrow 1 - \widetilde{g}_1(n) e^{\sqrt{\widetilde{\delta}_1(n)}\tau} > 0.$$

When $\widetilde{\delta}_1(n) = 0$, the equivalent condition for $e^{\widetilde{C}_1(\tau,n)v_1}$ to be bounded is $2 + \widetilde{b}_1(n)\tau \neq 0$.
Case 4. $\widetilde{b}_1(n) \geq 0$; then $2 + \widetilde{b}_1(n)\tau \geq 2$;
Case 5. $\widetilde{b}_1(n) < 0, -\widetilde{b}_1(n)\tau < 2$; then $0 < 2 + \widetilde{b}_1(n)\tau < 2$.
When $\widetilde{\delta}_1(n) < 0$, the equivalent condition for $e^{\widetilde{C}_1(\tau,n)v_1}$ to be bounded is

$$\frac{\sqrt{-\widetilde{\delta}_1(n)}}{2}\tau - \arctan \frac{\widetilde{b}_1(n)}{\sqrt{-\widetilde{\delta}_1(n)}} \neq \frac{\pi}{2}.$$

Case 6. $\frac{\pi}{2} + \arctan \frac{\widetilde{b}_1(n)}{\sqrt{-\widetilde{\delta}_1(n)}} > \frac{\sqrt{-\widetilde{\delta}_1(n)}}{2}\tau$; then

$$-\frac{\pi}{2} < \frac{\sqrt{-\widetilde{\delta}_1(n)}}{2}\tau - \arctan \frac{\widetilde{b}_1(n)}{\sqrt{-\widetilde{\delta}_1(n)}} < \frac{\pi}{2}.$$

In the same line, the conditions of $e^{\widetilde{C}_2(\tau,n)v_2}$ and $e^{\widetilde{D}(\tau,n)r}$ can be derived.
Now, concentrate on the boundedness of $e^{\widetilde{A}(\tau,n)}$. It is worth noting that its equivalent is that $E[e^{nJ_{01}}]$ and $E[e^{nJ_{11}}]$ are finite. Because J_{01} and J_{11} are separately subject to log-normal distribution and asymmetric double exponential distribution, we have

$$\begin{aligned} E[e^{nJ_{01}}] &= e^{n\mu_1 + \frac{1}{2}n^2\sigma_{J_{01}}^2}, \\ E[e^{nJ_{11}}] &= \tfrac{p_1\xi_1}{\xi_1+n} + \tfrac{q_1\eta_1}{\eta_1-n}, -\xi_1 < n < \eta_1. \end{aligned}$$

The proof is finished. □

Appendix: The proof of Lemma 2.3.

Proof. Because of the conditions $B^2 - 4AC \neq 0$, obviously, the inequality $y_1 \neq y_2$ holds. Furthermore, at least one of y_1 and y_2 is not equal to E. Let us assume that $y_2 \neq E$. Because

$$Ay^2 + By + C = A(y - y_1)(y - y_2),$$

when $y \neq y_1, y_2$,

$$\frac{1}{(y - y_1)(y - y_2)}\mathrm{d}y = A\mathrm{d}x,$$

when $y \neq 0$. Integrating both sides of the equation gives

$$\frac{1}{y_1 - y_2} \ln \frac{y - y_1}{y - y_2} = Ax + D.$$

Here, D is a constant. From the above equation, we can obtain

$$\frac{y-y_1}{y-y_2}=\mathrm{e}^{D(y_1-y_2)}\mathrm{e}^{Ax(y_1-y_2)}.$$

Let $c=\mathrm{e}^{D(y_1-y_2)}$. Considering that $A(y_1-y_2)=d$, then

$$\frac{y-y_1}{y-y_2}=c\mathrm{e}^{dx}.$$

Therefore, we can obtain

$$y=\frac{y_1-y_2c\mathrm{e}^{dx}}{1-c\mathrm{e}^{dx}}.$$

Because $y_2\neq E$, it follows that $y=y_2$ is not a solution to the above equation . If $c=0$ is allowed, then when $c=0$, $y=y_1$, so this equation is the general solution of differential equations. Using the initial condition $y|_{x=0}=E$, we can solve for the constant $c=\frac{E-y_1}{E-y_2}$. Substituting this into this equation gives the solution to differential equations as

$$y=\frac{y_1-\frac{E-y_1}{E-y_2}y_2\mathrm{e}^{dx}}{1-\frac{E-y_1}{E-y_2}\mathrm{e}^{dx}}=\frac{(E-y_2)y_1-(E-y_1)y_2\mathrm{e}^{dx}}{E-y_2-(E-y_1)\mathrm{e}^{dx}}.$$

The lemma has been proved. □

Appendix: The positivity conditions for v_{1t}, v_{2t}, and r_t

Based on the research approach of [34], taking v_{1t} as an example in Table 20, we will present the positive conditions.

Table 20. The positive condition of the volatility factor v_{1t}.

Value	Process name	Positive condition	Explanation
$\alpha=0$	OU	Impossible to be positive	Constant diffusion, must be negative
$0<\alpha<\frac{1}{2}$	quadratic root	$k_1>0,\theta_1>0,\sigma_1>0$	0 is an unreachable boundary
$\alpha=\frac{1}{2}$	CIR	$2k_1\theta_1>\sigma_1^2, k_1>0,\theta_1>0,\sigma_1>0$	Classic Feller condition
$\frac{1}{2}<\alpha<1$	super square root	$k_1>0,\theta_1>0,\sigma_1>0$	0 is an unreachable boundary
$\alpha=1$	MR-GBM	$k_1>0,\theta_1>0,\sigma_1>0$	0 is an unreachable boundary

If $\alpha<\frac{1}{2}$, the diffusion term decays more rapidly near the origin compared to the drift term (that is, the drift term dominates), so the positivity is automatically guaranteed. If $\alpha>\frac{1}{2}$, the diffusion term decays more slowly near the origin compared to the drift term (meaning the random fluctuations are greater), but at this time, the drift term is k_1. As the constant term, it provides sufficient "thrust" at $v=0$, thus ensuring positivity automatically.